

**Polymerization of Ethylene using
Metallocene and Zeigler Natta catalyst with
doped-Nanotitania**

ABDUL KALEEL SULAIMAN HANIFFA

CHEMICAL ENGINEERING

May 2011

**Polymerization of Ethylene using
Metallocene and Zeigler Natta catalyst with
doped-Nanotitania**

BY

ABDUL KALEEL SULAIMAN HANIFFA

A Thesis Presented to the
DEANSHIP OF GRADUATE STUDIES

KING FAHD UNIVERSITY OF PETROLEUM & MINERALS

DHAHRAN, SAUDI ARABIA

In Partial Fulfillment of the
Requirements for the Degree of

MASTER OF SCIENCE

In

CHEMICAL ENGINEERING

May 2011

KING FAHD UNIVERSITY OF PETROLEUM & MINERALS
DHAHRAN 31261, SAUDI ARABIA

DEANSHIP OF GRADUATE STUDIES

This thesis, written by Abdul Kaleel Sulaiman Haniffa under the direction of his thesis advisor and approved by his thesis committee, has been presented to and accepted by Dean of Graduate Studies, in partial fulfillment of the requirements for the degree of **MASTER OF SCIENCE** in **CHEMICAL ENGINEERING**.

Thesis Committee



Dr. Mamdouh Al-Harhi (Advisor)



Dr. Sadhan Kumar De (Co-Advisor)



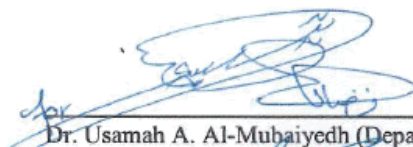
Dr. Bijal Kottukkal Bahuleyan (Member)



Dr. Reyad A. Shawabkeh (Member)



Dr. Rachid Sougrat (Member)



Dr. Usamah A. Al-Muhaiyedh (Department Chairman)

Dr. Salam Adel Zummo (Dean of Graduate Studies)

Date

24/7/11



Dedicated

to

my beloved parents and family members

Acknowledgements

Verily all praise is due to Allah (ﷻ). We praise Him; we seek His help and forgiveness. Peace and blessings be upon Prophet Muhammad (ﷺ), the last of Allah's Messengers and Prophets, and upon his family, his Companions and all those who follow in his footsteps until the end of time. I would like to express my deepest gratitude to my parents and all my family members for their love, prayers, constant support and encouragement.

I acknowledge the support and facilities provided by King Fahd University of Petroleum & Minerals (KFUPM). I would like to express my sincere gratitude to my thesis advisor Dr. Mamdouh Al-Harthi for his guidance, support and invaluable advice through-out this thesis. I also thank my committee members Dr. S.K. De (co-advisor), Dr. Bijal.K.B, Dr. Reyad A. Shawabkeh and Dr. Rachid Sougrat (KAUST) for their feedback, support and advice given during this thesis work.

I am also thankful the chairman of Chemical Engineering Department, Dr. Usamah Al-Mubaiyedh for his cooperation and providing department facilities.

I also thank all my fellow graduate students and all my friends who made this an enjoyable experience.

Table of Contents

Table of Contents	vii
Table of Figures.....	ix
List of Tables	xiii
Thesis Abstract.....	xiv
ملخص الرسالة	xv
Chapter 1	1
Introduction.....	1
Chapter 2	6
Literature Survey	6
2.1 Polymer Filled Nanocomposites	6
2.2 Nanotitania as filler	7
2.3 Metallocene Catalyst	9
2.4 Ziegler-Natta Catalyst	14
2.5 Synthesis of Polymer nanocomposites	16
Chapter 3	18
Project Objectives	18
Chapter 4	19
Experimental Methods	19
4.1 Materials.....	19
4.2 Characterization	19
4.2.1 Thermal analysis of the samples	20
4.2.2 CRYSTAF.....	20
4.3 Polymerization	21
4.3.1 Synthesis of PE-Doped TiO ₂ Nanocomposites at low pressure.....	21
4.3.2 Synthesis of PE-Doped TiO ₂ Nanocomposites at High pressure.....	21

Chapter 5.....	23
Results and Discussion	23
5.1Effect of Filler Concentration on the activity of the catalyst and polymer properties	23
5.2Effect of Polymerization Conditions on Catalyst Activity and Polymer Properties .	31
5.3 Effect of Filler concentration & Polymerization time on the thermal properties of polymer.....	39
5.4.Effect of Polymerization Conditions on Thermal Properties of Polymer	51
5.5Effect of catalyst substituent group on the catalyst activity and thermal properties of polymer in the presence of filler	60
5.6Effect of Polymerization Conditions on the catalyst activity and thermal properties of polymer in the presence of filler	68
5.7Effect of filler on activity of Zeigler Natta Catalyst and polymer properties	74
Chapter 6.....	76
Conclusion and Future Work.....	76
6.1.Future Research.....	77
Bibliography.....	78
Curriculum Vita	82

Table of Figures

Figure 1-1: Materials selection requirements for thermoplastic nanocomposites	2
Figure 1-2: Titanium Dioxide attributes and applications	5
Figure 2-1: Reaction mechanism of zirconocenes with MAO.	13
Figure 5-1: Activity of synthesized polyethylene nanocomposites using polymerization time of 30 mins at 30°C at 1 bar ethylene pressure.....	26
Figure 5-2: SEM micrographs of (a) Control (Entry 1, Table1) (b) Polyethylene with 15 mg of TiO ₂ /Mn using polymerization time of 30 mins (Entry 3, Table1) (c) Higher magnification of polyethylene with 15 mg of TiO ₂ /Mn using polymerization time of 30 mins (Entry 3, Table1) (d) Polyethylene prepared using polymerization time of 120 mins (Entry 8, Table1).....	29
Figure 5-3: TEM micrographs of (a) Control (Entry 1, Table1) (b) Polyethylene with 15 mg of TiO ₂ /Mn (Entry 3, Table1)	30
Figure 5-4: WAXD patterns of doped-TiO ₂ (BK 0), Control (BK 20), and PE/doped-TiO ₂ nanocomposites (BK 16, BK 17 & BK 5)	31
Figure 5-5: Polymerization activity of metallocene (Zr - Cp ₂ ZrCl ₂ , Ti - Cp ₂ TiCl ₂) to form polyethylene nanocomposites (Temperature-30°C, Time-30 mins, and Ethylene pressure-1 bar).....	32
Figure 5-6: Polymerization activity of metallocene (Zr - Cp ₂ ZrCl ₂ , Ti - Cp ₂ TiCl ₂) to form polyethylene nanocomposites (Temperature-60°C, Time-30 mins, and Ethylene pressure-1 bar).....	33
Figure 5-7: Polymerization activity of metallocene (Zr - Cp ₂ ZrCl ₂ , Ti - Cp ₂ TiCl ₂) to form polyethylene nanocomposites (Temperature-30°C & 60°C, Time-30 mins, and Ethylene pressure-1 bar)	34
Figure 5-8: Effect of temperature on the polymerization activity of the metallocene(Zr - Cp ₂ ZrCl ₂ , Ti - Cp ₂ TiCl ₂) to form polyethylene nanocomposites (Time-30 mins, Ethylene pressure – 1 bar)	35

Figure 5-9: Effect of pressure on the activity of the catalyst ($\text{Zr} - \text{Cp}_2\text{ZrCl}_2$), here Zr-C represents the Control and other two represents the nanocomposites with filler at 30°C with reaction time of 30 mins	37
Figure 5-10: Effect of time on the activity of the catalyst($\text{Zr} - \text{Cp}_2\text{ZrCl}_2$) with reaction time of 30 mins at 30°C at 5 bat ethylene pressure.	38
Figure 5-11: DSC second heating curves of homopolymer, polyethylene with doped-titania (15 mg) synthesized using Cp_2ZrCl_2 catalyst	41
Figure 5-12: DSC second heating curves of polyethylene with doped-titania using different concentrations of filler with Cp_2ZrCl_2 catalyst.....	41
Figure 5-13: DSC second heating curves of polyethylene with different fillers with Cp_2ZrCl_2 catalyst	43
Figure 5-14: DSC second heating curves of polyethylene with different polymerization time with Cp_2ZrCl_2 catalyst	43
Figure 5-15: DSC second heating curves of homopolymer, polyethylene with doped-titania (15 mg) synthesized using Cp_2TiCl_2 catalyst	44
Figure 5-16: CRYSTAF analysis of polymer nanocomposite obtained by Cp_2ZrCl_2 catalyst; a) in the absence of doped-titania b) in the presence of doped-titania. (Temperature- 30°C , Ethylene Pressure-1 bar, Time-30mins)	45
Figure 5-17: CRYSTAF analysis of polymer nanocomposite obtained by Cp_2ZrCl_2 catalyst at different concentrations of filler (Temperature- 30°C , Ethylene Pressure-1 bar, Time-30mins)	45
Figure 5-18: CRYSTAF analysis of polymer nanocomposite obtained by Cp_2ZrCl_2 catalyst at optimal concentration of filler by varying the reaction time (Filler concentration-15 mg, Temperature- 30°C , Pressure-1 bar)	46
Figure 5-19: TGA curves of homopolymer, polyethylene with doped-titania, polyethylene with pure titania and polyethylene with pure manganese oxide synthesized using Zirconocene catalyst.....	47

Figure 5-20: TGA curves of homopolymer and polyethylene with doped-titania at different filler concentrations using Zirconocene catalyst	48
Figure 5-21: TGA curves of homopolymer and polyethylene with doped-titania synthesized by varying the reaction time using Zirconocene catalyst	49
Figure 5-22: TGA curves of homopolymer and polyethylene with doped-titania synthesized using Titanocene catalyst	50
Figure 5-23: DSC second heating curves of homopolymer synthesized at high temperature, polyethylene with doped-titania synthesized at high temperature and low temperature using Zirconocene.	53
Figure 5-24: TGA curves of polyethylene with doped-titania synthesized at different polymerization temperatures using Zirconocene catalyst	53
Figure 5-25: TGA curves of polyethylene with doped-titania synthesized at high temperature using different catalysts.	54
Figure 5-26: DSC second heating curves of homopolymer, polyethylene with doped-titania synthesized at high pressure using Zirconocene catalyst	56
Figure 5-27: DSC second heating curves of polyethylene with doped-titania synthesized at high pressure by varying the reaction time using Zirconocene catalyst	57
Figure 5-28: TGA curves of homopolymer and polyethylene with doped-titania synthesized at high pressure (5 bar) using Zirconocene catalyst	57
Figure 5-29: TGA curves of polyethylene with doped-titania synthesized at high pressure (5 bar) using Zirconocene catalyst	58
Figure 5-30: Activity of synthesized polyethylene nanocomposites using polymerization time of 30 mins at 30°C in presence of (B-Zr = (BuCp) ₂ ZrCl ₂ , Ter-B-Zr = (t-BuCp) ₂ ZrCl ₂).	61
Figure 5-31: DSC second heating curves of homopolymer, polyethylene with doped-titania synthesized using butyl-Zirconocene catalyst	63

Figure 5-32: DSC second heating curves of homopolymer, polyethylene with doped-titania synthesized using ter-butyl-Zirconocene catalyst.....	64
Figure 5-33: DSC second heating curves of polyethylene with doped-titania synthesized using butyl and ter-butyl-Zirconocene catalyst	64
Figure 5-34: TGA curves of homopolymer, polyethylene with doped-titania synthesized using butyl-Zirconocene catalyst.....	65
Figure 5-35: TGA curves of homopolymer and polyethylene with doped-titania synthesized using ter-butyl-Zirconocene catalyst.....	66
Figure 5-36: TGA curves of polyethylene with doped-titania, synthesized using butyl and ter-butyl-Zirconocene catalyst	67
Figure 5-37: Activity of synthesized polyethylene nanocomposites using polymerization time of 30 mins at 60°C in presence of (B-Zr = (BuCp) ₂ ZrCl ₂ , Ter-B-Zr = (t-BuCp) ₂ ZrCl ₂).	69
Figure 5-38: DSC second heating curves of homopolymer synthesized at high temperature, polyethylene with doped-titania synthesized at high temperature and low temperature using butyl-Zirconocene catalyst	70
Figure 5-39: DSC second heating curves of homopolymer synthesized at high temperature, polyethylene with doped-titania synthesized at high temperature and low temperature using butyl-Zirconocene catalyst	71
Figure 5-40: TGA curves of polyethylene with doped-titania synthesized at different polymerization temperatures using Butyl-Zirconocene catalyst	72
Figure 5-41: TGA curves of polyethylene with doped-titania synthesized at different polymerization temperatures using ter-Butyl-Zirconocene catalyst	72
Figure 5-42: Activity of synthesized polyethylene nanocomposites using polymerization time of 30 mins at different temperatures in presence of Zeigler-Natta catalyst.	75

List of Tables

Table 2-1: Polymerization Activity of $\text{Cp}_2\text{ZrCl}_2/\text{MAO}$ (Temperature-95°C, Pressure-8 bar)	11
Table 5-1: Experimental conditions and properties of polyethylene prepared by insitu polymerization using Cp_2ZrCl_2 & Cp_2TiCl_2 catalyst and Methyl aluminoxane co-catalyst system.....	25
Table 5-2: Experimental conditions and properties of polyethylene prepared by insitu polymerization using Cp_2ZrCl_2 & Cp_2TiCl_2 catalyst and Methyl aluminoxane co-catalyst system.....	32
Table 5-3: Experimental conditions and properties of polyethylene prepared by insitu polymerization using Cp_2ZrCl_2 catalyst and Methyl aluminoxane co-catalyst system.	36
Table 5-4: Experimental conditions and properties of polyethylene prepared by insitu polymerization using Cp_2ZrCl_2 & Cp_2TiCl_2 catalyst and Methyl aluminoxane co-catalyst system.....	40
Table 5-5: Experimental Conditions and properties of polyethylene prepared by insitu polymerization using Cp_2ZrCl_2 & Cp_2TiCl_2 catalyst and Methyl aluminoxane co-catalyst system.....	51
Table 5-6: Experimental Conditions and properties of polyethylene prepared by insitu polymerization using Cp_2ZrCl_2 catalyst and Methyl aluminoxane co-catalyst system.	55
Table 5-7: Ethylene polymerization results at High pressure. ^a	59
Table 5-8: Experimental Conditions and properties of polyethylene prepared by insitu polymerization using $(\text{BuCp})_2\text{ZrCl}_2$ & $(\text{t-BuCp})_2\text{ZrCl}_2$ catalyst and Methyl aluminoxane co-catalyst system.	62
Table 5-9: Experimental Conditions and properties of polyethylene prepared by insitu polymerization using Cp_2ZrCl_2 & Cp_2TiCl_2 catalyst and Methyl aluminoxane co-catalyst system.....	68
Table 5-10: Experimental Conditions and properties of polyethylene prepared by insitu polymerization using TiCl_4 catalyst and Triisobutyl aluminum co-catalyst system.....	74

THESIS ABSTRACT

Name: Abdul Kaleel Sulaiman Haniffa

Title: Polymerization of Ethylene using Metallocene and Zeigler Natta catalyst with doped-Nanotitania

Major Field: Chemical Engineering

Date of Degree: May-2011

Ethylene polymerization was carried out using highly active metallocene catalysts (Cp_2ZrCl_2 and Cp_2TiCl_2) in combination with methylalumoxane. Titanium (IV) oxide containing 1% Mn as dopant was used as nanofillers. The influence of filler concentration, reaction temperature and pressure on the catalytic activity and polymer properties was investigated. There was a four-fold increase in the activity of zirconocene catalyst by addition of doped-titania. The morphology indicates that the doped-titania nanoparticles have a nucleus effect on the polymerization and caused a homogeneous PE shell around them. The optimum condition for polymerization was found to be 30oC. The improvement of nanoparticles dispersion in the polyethylene matrix was checked by WAXD. The thermal properties were analyzed using differential scanning calorimetry and thermogravimetric analysis. A detailed investigation on the polymerization of ethylene by Cp_2ZrCl_2 catalysts was carried out by varying the cyclopentadienyl substituent groups. The activity of catalyst in comparison to the Cp_2ZrCl_2 was low due to the steric effect from the substituent groups even in the presence of filler.

ملخص الرسالة

الاسم: عبد الخليل سليمان حنيفة

العنوان: بلمرة الإيثيلين باستخدام وسيط الميثلوسين زيغلر-ناتا المدعمة بالدوبد نانوتيتانيا

التخصص: الهندسة الكيميائية

تاريخ الحصول على الدرجة: مايو 2011م

لقد تم بلمرة الإيثيلين باستخدام وسيط المادة المحفزة الميثلوسين النشط بدرجة عالية (Cp_2TiCl_2 , Cp_2ZrCl_2) بالاتحاد مع الميثيللوموكسان. ولقد تم استخدام أكسيد التانتاليوم (IV) والذي يحتوي علي (1% من ممستحضر ام ان) كنانوفيلر. كما تم دراسة تأثير تركيز الحشو (الفيلر)، رد الفعل الحراري، والضغط على نشاط المادة المحفزة وخصائص البلمرة. فلقد كان هناك زيادة بمقدار أربعة أضعاف في نشاط وسيط الزيركونوسين بإضافة مادة (doped-titania). وقد أوضحت المورفولوجي أن النانوبرتيكلر دوبد تيتنيا (doped-titania nanoparticles) لها تأثير مركزي على البلمرة وقد تسببت في ظهور قوقعة (PE) متجانسة حولهم. إن الظروف المثالية لعملية البلمرة هي (30) درجة. ولقد تم التأكد من تحسين تشتت النانوبرتيكلر في ماتريكس البولي إيثيلين باستخدام (WAXD). كما تم تحليل الخصائص الحرارية باستخدام المسعر الحراري التبايني والتحليل الوزني الحراري. وقد تم عمل فحص مفصل على بلمرة الإيثيلين باستخدام المادة المحفزة الوسيطة (Cp_2ZrCl_2) من خلال تغيير المجموعات المستبدلة من السايكلوبنتادانيل. ولقد كان نشاط المادة المحفزة الوسيطة مقارنة بـ (Cp_2ZrCl_2) منخفضاً نظراً للتأثير التجسيمي الناشئ من المجموعات المستبدلة بالرغم من وجود الحشوة (فيلر).

Chapter 1

Introduction

Polyolefins are the most common commercial polymers, being used in our day to day life but due to many unavoidable reasons prevents their wider use. Polymer nanocomposites are a unique new class of materials with an ultrafine dispersion of nanomaterials in a polymeric matrix. They show unique properties by combining the unique properties of the inorganic nanofillers (e.g., thermal stability, rigidity) and the organic polymers (e.g., dielectric conductivity, flexibility, processability and ductility) [1]. Various inorganic nanofillers such as silicon dioxide (SiO_2) [2–5], titanium dioxide (TiO_2) [6–9], Aluminium trioxide (Al_2O_3) [10, 11], and Zinc oxide (ZnO) [12, 13] have been used to improve polymer properties. Innovative composites and nanocomposites are significantly widening the range of applications of thermoplastics as well as thermosets in areas such as packaging, automotive, bio-medical devices, electronics etc. The focus is to disperse nanofillers in polymer matrix and study its effect on the activity of ethylene polymerization and morphological characteristics of the synthesized polymer.

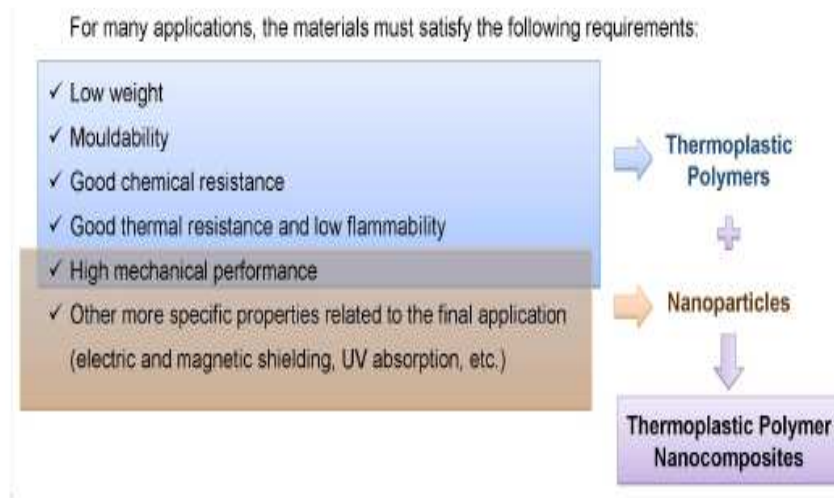


Figure 1-1: Materials selection requirements for thermoplastic nanocomposites.

Nanoparticles are defined as particles with diameters below the micron dimension: generally, below $0.1\ \mu\text{m}$ (100 nm). To be more accurate, nanoparticles are particles with properties depending directly on their size. Examples are optical, electrical, or magnetic properties. Therefore, in many cases the latter definition restricts nanoparticles to particles with sizes below 10–20 nm. The surface properties are said to be crucial, thus with decrease in particle size, the ratio of surface/volume increases. The dependency of surface/volume ratio is a function of size. In this context, it is important to realize that e.g., 5 nm particles consist of only a few 1000 atoms or unit cells and possess approximately 40% of their atoms at the surface. In contrast, $0.1\ \mu\text{m}$ particles contain some 10⁷ atoms or unit cells, and only 1% of their atoms are located at the surface. Therefore, the smaller the particles are, the more important will be surface properties, influencing interfacial properties, agglomeration behavior, and also - as will be shown later - physical properties of the particles. As the surface area of nanoparticles is some $100\ \text{m}^2/\text{g}$, contaminations stemming from the various synthesis processes, as e.g., remaining precursor residuals, or solvents,

may additionally influence the surface properties [14]. Three main constituents of material in any composite are the interfacial region, the reinforcement (fiber) and matrix. The communication between the filler and the matrix depends on interfacial region and because of its proximity to the filler surface; the interfacial region is conventionally ascribed properties different from the bulk matrix [15]. The current micromechanics theories [16] suggest that the effective properties of polymer microscale filled composites rely on components volume fraction, shape, constituents and filler arrangement, and interface between filler and polymer. Based on the previous suggestion, properties of polymer composites are thus independent of the size of fillers. Obviously, this may not be correct for polymer nanocomposites. The most prominent difference of nanocomposites compared with their traditional counterparts is the small size of the fillers, which could bring added specific phenomena. For example, nanotube fillers possess strength as high as 500 GPa and modulus as high as 1 TPa. Nanoparticles are optically active and do not scatter light significantly, which can be combined into a polymer to obtain the optical gain of the material. The ductility of the polymer is not affected to the great extent by the use of very small fillers as these fillers do not build large stress concentration. Novel materials with enhanced thermal stability, chemical resistance, scratch resistance, mechanical property, ion conductivity and flame retardancy, can be obtained by dispersing the inorganic nanoparticles in the polymer matrices [17, 18].

The small decrease in size of the fillers less than 100 nm leads to dramatically augmented interfacial area per unit volume or weight of the dispersed phase, which control the degree of interaction between the polymer and filler phase and thus controls the properties. Hence, the greatest challenge in making polymer nanocomposites is to

learn how to control the interface. The bulk polymers are converted to interfacial polymers by addition of nanoparticles and these polymers exhibit different properties. Major changes can be brought in the polymer properties just by adding small amount of nanoparticles because of their low percolation threshold. The homogeneous dispersion of nanofillers within the polymer matrix is very crucial to explore the full potential of nanocomposites. To realize the novel properties of polymer nanocomposites, synthetic methods which have effect on controlling particle size distribution, dispersion, and interfacial interactions are critical. Generally, three ways have been applied to disperse nanopowders in polymers. The first is direct mixing or blending of the polymer and the nanopowder either as discrete phases (known as melt mixing) or in solution (solution mixing). The second is sol-gel process which starts with molecular precursor at ambient temperature and then forms metal or metal oxide framework by hydrolysis and condensation. The third is in situ grafting polymerization of macromolecular chains on the surface of nanopowder.

High refractive index of titanium dioxide is the main reason for preferring TiO_2 nanoparticles and these nanoparticles have low toxicity and low cost as a bulk material [19]. Titanium dioxide (TiO_2) is a multifaceted material when used in polymer applications. The application of titanium dioxide which is well known to the people is the leading white pigment. However, TiO_2 brings more to the polymer industry than just white, bright opacity. Titanium dioxide adds value to the material by its interaction with light because it is photo-responsive in nature. For example, this interaction could be the absorption of ultraviolet light energy, in this manner it protects the polymer from UV degradation or it can be the familiar scattering that results in opacity.

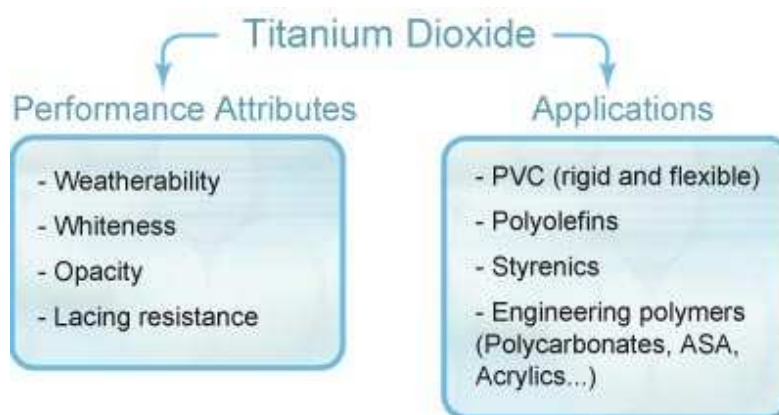


Figure 1-2: Titanium Dioxide attributes and applications

Titanium dioxide based photocatalysis technology is currently at the commercialization stage in many industries. Titanium dioxide effectiveness (rate of photocatalytic reaction) can be intensified by modifying its surface with noble metal deposition.. The purpose of doping TiO_2 nanoparticles with metals is to create a heterojunction – a space which ranges from 10 to 100 nm in size, located between the surface of the doping metal and that of the TiO_2 nanoparticle. The applications for doped TiO_2 nanocomposites range from antimicrobial coatings on textiles, the inactivation of endospores, solid - surface antimicrobial coatings, and aqueous system - based biocides.

In this study, ethylene polymerization will be carried out in presence of Manganese doped-titania and its effect on polymerization activity and its impact on the various property of the polymer will be studied.

Chapter 2

Literature Survey

2.1 Polymer Filled Nanocomposites

Conventional polymer composites, usually reinforced by micrometer-scale fillers into polymer matrices, have found large-scale applications for decades in automobile, construction, electronics, and consumer products. There is an enhancement in the various properties of the composites such as higher strength and stiffness compared with neat polymer [20-22]. However, achievement of these properties by the traditional composites involves compromises. For example, stiffness is obtained at cost of toughness, which is also traded for optical clarity. Recently, nanoparticle filled polymer composites give a new way to overcome the limitations of traditional counterparts. An idea suggested by current micromechanics theories [23] is that the effective properties of polymer microscale filled composites rely on constituents, volume fraction of components, shape and arrangement of fillers, and polymer/filler interface.

The most prominent difference of nanocomposites compared with their traditional counterparts is the filler size itself, which could bring added specific phenomena. For example, the strength of nanotube fillers is said to be 500 GPa with modulus of 1 TPa. The polymer can be combined with optically active nanoparticles which enhances the optical gain

of the material. The ductility of the polymer is not affected by addition of small fillers as they don't build large stress concentrations. In addition, filler size less than 100 nm leads to dramatically augmented interfacial area per unit volume or weight of the dispersed phase, which control the degree of interaction between the polymer and filler phase and thus affect the polymer properties. Hence, the control of interface places a crucial role in the making of polymer nanocomposites.

To realize the novel properties of polymer nanocomposites, synthetic methods which have effect on controlling dispersion, interfacial interactions and particle size distribution are very important. Nanocomposites synthetic techniques are quite different and creating one universal technique for developing polymer nanocomposites is impossible due to the physiochemical differences between each system. Each polymer system may require a special set of processing conditions to be formed and different synthetic techniques in general could yield nonequivalent results [24].

2.2 Nanotitania as filler

Early studies show that TiO_2 was used mostly as a pigment than as filler for improving mechanical strength. Nussbaumer et al., [6] utilized TiO_2 due to its photo-responsive properties to synthesis polymer nanocomposites to produce high refractive index materials by solution mixing technique.

Polymers such as polyvinyl alcohol, polyvinylpyrrolidone and poly (4-vinylpyridine) were used to produce films using rutile TiO_2 . These studies concluded that the TiO_2 was well dispersed in the polymer and showed strong UV absorbance absorption with a maximum at 225nm and with a high extinction coefficient and a small full width at half maximum.

Another interesting aspect was determined at high loading rates of TiO_2 ; they found that from the acquisition limit of 180 nm (instrumental limit) up to 360 nm the Ultra violet radiation was almost absorbed. Thus, from these findings they have suggested that these samples can act as optically efficient UV filters.

In the recent past, efforts to utilize titania to enhance overall polymer properties have gained a major momentum. It have been reported that the TiO_2 filled polymers prepared by met-compounding shows a significant improvement in the properties over homopolymers and micron-sized particle-filled polymer composites [25–31]. Different kinds of polymer-based TiO_2 composites have been reported in the literature, such as high impact polystyrene (HIPS)/nano- TiO_2 [32] and polyamide/nano- TiO_2 composite [33]. However titania filled polyolefins will be the focus of our discussion.

Wang et al., [34] in 2005 prepared and characterized TiO_2 filled polyethylene composite/polymer. The group used two-step melt compounding using an extruder to produce TiO_2 filled polyethylene composites. They prepared a master batch at a 20% ratio of TiO_2 . The prepared master batch of LDPE/ TiO_2 (20 wt %) was diluted with different amounts of PE in an extruder to obtain different compositions of TiO_2 . They analyzed the polymer for its rheological, mechanical and dispersion properties of TiO_2 in the polymer. They concluded that the introduction of TiO_2 increased the viscosity of composites and produced a better dispersion of TiO_2 in the melt-compounding. The Mechanical tests showed that, compared with neat PE, the notched impact strength and tensile strength were improved by about 45% and 5%, respectively, with the incorporation of only 2 wt% TiO_2 . SEM observation of the fracture surfaces also indicated that the nanocomposites exhibited a stronger ductile fracture behavior than neat PE.

Supaphol et al., [35] in 2007, reported the effect of variation in the surface characteristics of titanium dioxide such as neat TiO_2 , stearic acid-coated TiO_2 and silica (SiO_2)-coated TiO_2 and the filler concentration (ranging from 5 to 30wt%) on subsequent melting behavior, mechanical properties and non-isothermal melt-crystallization of filled isotactic polypropylene (iPP). The group followed a direct blending technique for preparing PP filled TiO_2 polymers using an extruder for meltblending. They concluded that the crystallization exotherm became larger for these samples and there was a shift towards a lower temperature with the increase in cooling rate. There was an increase in the peak crystallization temperature (T_p) for the iPP samples filled with neat TiO_2 nanoparticles compared to the homopolymer and there was not much impact by varying the filler concentration. In the case, isotactic polypropylene filled with stearic acid-coated TiO_2 nanoparticles, there was no significant difference in the T_p values when compared to the neat iPP. But marked difference in the T_p values for iPP samples filled with 5, 20, and 30 wt% SiO_2 -coated TiO_2 nanoparticles was reported in comparison with the neat isotactic polypropylene. Lastly, the presence of the TiO_2 enhances the rigidity of the resulting composites.

2.3 Metallocene Catalyst

Methylaluminoxane activated metallocenes and other transition metal complexes which have high polymerization activity of Styrene, olefins and diolefins was discovered at the University of Hamburg about three decades ago. High activity of metallocene/methylaluminoxane is well known in the synthesis of specifically premeditated polyolefins and engineering plastics [36].

To be specific, zirconocene and titanocene complexes have opened a frontier in the area of synthesis of polymer and its processing. Methylaluminoxane and other bulky cocatalysts like perfluorophenylborate are used to activate transition metal complexes. The tailoring of microstructure tacticity and stereo regularity of the synthesized polymers are carried out by ligand structure which also influence the superior properties of copolymers such as lower extractables, tensile strength and film clarity. There is an enhancement in the chemical and physical properties of the composite materials when these materials are synthesized by in-situ polymerization in the presence of single-site catalyst in combination with efficient filler pretreatment. For example, considerable flame retardancy, significant enhancement of stiffness without compromising much in the case of impact strength, improvement in gas barrier properties, high crystallization rates as well as better gloss and clarity were observed. Low nanoparticle contents are adequate enough to attain novel or tailored material characteristics such as Crystallization behavior. During the polymer processing these crystallization behaviors such as the melting temperature (T_m), crystallization temperature (T_c), and the half-time of crystallization ($\tau_{0.5}$) plays a vital role. The cycle times can be shortened by reducing the cooling time essential for part solidification. By incorporating nucleating agents into the neat polymer results in shorten cycle times and it also speeds up the crystallization. The morphology is influenced by crystallization kinetic, which in turn affects the physical and mechanical properties of a semi-crystalline polymer like Polypropylene and Polyethylene [37, 38]. The main difference between the conventional Ziegler-Natta catalysts and metallocene catalysts is the active site distribution. Heterogeneous Ziegler-Natta catalysts have many active sites of which some are stereospecific, and some are more accessible to monomers for coordination and subsequent polymerization.

On the other hand, metallocene are homogeneous and each molecule has the same activity as they are accessed by same amount of monomers. The resulting product is very uniform and highly stereoregular with alpha-olefins. These catalysts are said to be single site catalysts (SSC). These catalysts allow a more regular distribution of comonomers along the backbone of polyethylene resulting in: 1) the incorporation efficiency (the total amount of comonomer consumed), leading to reduction in the comonomer required to give a designated density, and 2) the reduction in the amount of comonomer lost in the recycle purge stream which is referred as recovery efficiency.

The activity of catalyst system comprising of Zirconocene/MAO was found to be higher than the conventional Ziegler-Natta catalyst. Forty million grams of polyethylene can be produced from the complex containing 1 g zirconium in 1 h of reaction time carried out at 95°C and 8 bar ethylene pressure (refer the below Table 2-1). Almost each and every zirconium atom acts as an active center by producing nearly forty six thousand polymer chains per hour. The insertion time of one ethylene unit is almost similar to the time of insertion observed for the enzyme synthesis i.e. 3×10^{-5} s.

Activity	39.8×10^6 g PE/g Zr x h
Zirconocene concentration	6.2×10^{-8} mol/L
MAO concentration (molecular weight 1200 g/mol)	7.1×10^{-4} mol/L
Molecular weight PE	78,000 g/mol
Polymerization degree	28,000
Formation time of one PE chain	0.087 s
Insertion time (Turnover) of ethylene	3.1×10^{-5} s

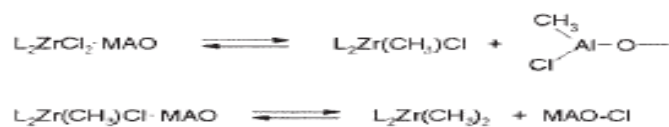
Table 2-1: Polymerization Activity of $\text{Cp}_2\text{ZrCl}_2/\text{MAO}$ (Temperature-95°C, Pressure-8 bar)

The significance in aging reactions of Ziegler–Natta catalysts resulted in the exploration and breakthrough of the metallocene/ MAO catalysts. The structure of MAO was found to be a complicated mixture of basic units. Hansjorg , from University of Hamburg, explored some structural aspect of the amorphous white powder. By investigating through various means such as NMR-measurements, decomposition reactions with HCl, alcohols, water and cryoscopic measurements in liquid trimethylaluminum or benzene, he concluded that methylaluminoxane consists of basic units of $\text{Al}_4\text{O}_3(\text{CH}_3)_6$. The combination of these units leads to the formation of cage structures of preferentially 4 units, which can be considered as the active form. The existence of bridging between methyl groups convinced Rytter that three units are sufficient. The rapid formation of metallocene/MAO complex was investigated by ultra-violet and infrared analysis (Figure 2-1). NMR and IR-experiments are used to investigate the alkylation. Many research showed that the metallocene catalyst activity depends on the cationic species formation. This statement is agreed by most of the research groups. The high excess of MAO required for polymerization and their function are not well clarified. There are two different explanations which illustrated the function of MAO. Firstly, α -Hydrogen transfer reactions from a zirconium methyl bond to a $-\text{CH}_3$ group of another zirconium complex or methylaluminoxane can occur in the system. High excess of methylaluminoxane is necessary to reactivate the inactive $\text{Zr-CH}_2\text{-Al}$ structure. Another explanation says that methylaluminoxane acts as a scavenger on impurities.

Complexation



Methylation



Activation



Deactivation



Reactivation

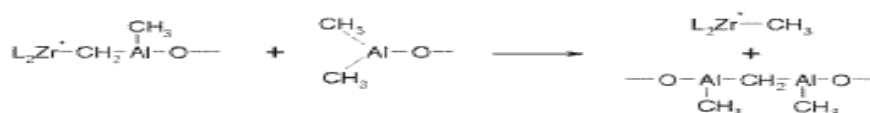


Figure 2-1: Reaction mechanism of zirconocenes with MAO.

Metallocene are very active soluble catalyst compared to the conventional heterogeneous Ziegler–Natta catalyst. Adsorption of these catalysts on the particles surface and fiber surface results in the uniform distribution of active sites. As methylaluminoxane is relatively stable against hydroxyl groups covering metal, biomass, or inorganic surfaces, the aluminoxane can be fixed without losing its activity. A thin polyolefin film is formed over the particles, after their treatment with metallocenes and addition of olefins. The thickness of polymer depends on the polymerization time. This procedure results in novel materials by combining the properties of fillers (eg. cellulose fibers, starch grains, metal powders, carbon fibers, silica monospheres, or nano-particles) with those of polyolefin resins.

2.4 Ziegler-Natta Catalyst

The Ziegler-Natta catalysts are being used in the polymer synthesis from the mid of twentieth century. Ziegler-Natta catalysts are based on a transition metal mixture, generally a titanium compound and an alkali metal such as Al_2O_3 . The activity of these catalyst systems is extremely high but less compared to the metallocene catalyst, variation in the physical properties are exhibited in their products [39-41]. The catalyst system is not clarified to a great extent till this day, but the monomers react through a number of reaction sites on the catalyst. Thus, most polymers exhibit broad molecular weight distribution when they are synthesized using heterogeneous Ziegler-Natta catalysts. There is a great interest in controlling the polymer chain length which triggers the investigation of new type of catalyst.

Most of the Ziegler-Natta polymerization reactions are based on titanium catalyst systems. There was an increase in the heterogeneous Ziegler-Natta catalytic activity when they are based on supported on activated MgCl_2 supported with TiCl_4 and it also helps in controlling the morphology of the product particles [42, 43]. Ziegler-Natta catalysts used for ethylene-propylene (EPM) or ethylene-propylene-diene (EPDM) rubbers production at industrial scale can be roughly classified into two families: the first family includes basically TiCl_3 , and the second family is the active form of magnesium chloride as a support for titanium compounds. In both cases, the support or solid catalyst need to be activated and transformed into the most active δ crystalline modification. The Ti atoms are found to be in small fraction in TiCl_3 which makes it less active, the potential active sites are the ones located at the catalyst crystallites surface.

Solvay efforts to increase the catalyst working surface led to the development of a further advanced, spheroidal catalyst for polypropylene, which was obtained by TiCl_4 reduction with AlEt_2Cl and subsequent electron donors (diisoamyl ethers or di-n-butyl) treatments, followed by a treatment with TiCl_4 .

Rong et al., [44] initiated the ethylene polymerization on the fiber surface by supporting TiCl_4 catalyst on the nanoscale crystal surface of palygorskite. Kwak et al., [45] reported that modified montmorillonite (MMT-OH) was first reacted with TiCl_4 at 30°C and then TiCl_4 was activated by introducing cocatalyst Et_3Al into the system. Complete exfoliation of MMT during Ti-based Ziegler-Natta polymerization has been effectively carried out, but uniform dispersion of clay was not achieved. Yang et al., [46] synthesized polyethylene nanocomposites using MMT/ MgCl_2 / TiCl_4 / AlEt_3 catalyst system. The nanoscale dispersion of montmorillonite in the polyethylene matrix was analyzed. There was a significant increase in the tensile strength was compared to that of homopolymer.

The roles of Ziegler-Natta catalyst in the polymer nanocomposite synthesis are numerous such as Ramazani [47] supported Ziegler-Natta catalyst on montmorillonite type clay for the first time and subsequently used for polymerizing ethylene. Further Ramazani [48] also reported the preparation of polypropylene/clay nanocomposites by MgCl_2 /MMT bisupported Ziegler-Natta catalyst, where montmorillonite acts as reinforcement agent and inert support. The results suggest that MMT silica layer in these polypropylene/clay nanocomposites were intercalated, partially exfoliated, and uniformly dispersed in the PP matrix. Huang et.al [49] synthesized polypropylene/graphene oxide (PP/GO) nanocomposites by in situ polymerization in the presence of Ziegler-Natta catalyst.

2.5 Synthesis of Polymer nanocomposites

Several dispersion routes into polymeric matrices have been described in the literature such as solution mixing, melt blending and insitu polymerization. However the melt blending technique has a major disadvantage being that host-guest incompatibilities usually result in nanoparticle aggregation and phase separation, which is detrimental to the polymer properties.

This has resulted the researchers for working on a better technique to minimize phase separation, aggregation and increase dispersion. Solution mixing is another technique that has been used to prepare metal oxide based polymer nanocomposites [50-52]. But the process does not suit polyolefins since the solubility of polyethylene (HDPE) and polypropylene in most low boiling organic solvents is very low. Another problem is the polyolefins are hydrophobic in nature and most of the inorganic fillers are hydrophilic in nature. This results in weak interfacial adhesion between polymer matrix and the filler and low mechanical properties. In-situ polymerization in the presence of metallocene catalysts can overcome these disadvantages. Kaminsky et al., reported the production of polyolefin nanocomposites by using metallocene-based catalysts treated filler surface [53-55]. Ross et al. [56] reported gas phase ethylene polymerization using SiO_2 supported $\text{rac-Me}_2\text{Si [Ind] 2ZrCl}_2$ / MAO at a temperature between 40 and 80°C where NaCl acts as a bed support and triethylaluminum (TEA) as a scavenger for impurities. Kumkaew et al., [57] has analyzed the gas-phase ethylene polymerization using mesoporous molecular sieves supported for zirconocene catalyst. Tannous and Soares [58] have also reported the effect of polymerization conditions on the gas-phase ethylene polymerization with SiO_2 supported Cp_2ZrCl_2 catalyst.

Guo et al., in 2006 was among the pioneers to produce linear low density polyethylene/titanium dioxide nanocomposites by in situ polymerization of ethylene/1-hexene using the $\text{Cp}_2\text{ZrCl}_2/\text{dMMAO}$ catalyst. They demonstrated the synthesis of high energy density isotactic polypropylene- BaTiO_3 and TiO_2 nanocomposites in situ metallocene polymerization. They used a two-step process wherein the initial step was to anchor the MAO onto the TiO_2 via surface hydroxyl group reaction to form covalent Al-O bonds. Later in situ polymerization was carried out with zirconocene catalyst [59]. Owpradit et al., had used various combinations of anatase and rutile forms of TiO_2 to assess the effect of different types of TiO_2 on the polymer properties [60]. He concluded that the anatase form increases the activity while rutile form was detrimental to the activity.

Recently, Owpradit et al., synthesized linear low density polyethylene TiO_2 nanocomposite using in situ polymerization with zirconocene/MAO catalyst. They impregnated the nanofillers with MAO to obtain MAO/ TiO_2 . Then, ethylene/1-hexene copolymerization was carried out using Cp_2ZrCl_2 catalyst in the presence of MAO/ TiO_2 . Their primary objective was to analyze the influence of crystalline regions on the polymer properties. The intrinsic activity in the presence of MAO/ TiO_2 (Anatase) was four times higher than the MAO/ TiO_2 (Rutile). The growth of TiO_2 as potential nanofillers has led researchers to use TiO_2 nanofillers in living radical polymerization [61]. The use of metallocene catalyst with titanium dioxide as nanofiller is an excellent combination to improve catalytic activity and polymer properties [62].

Chapter 3

Project Objectives

In this work, we have used nanotitania doped with 1% Mn to study the influence of manganese and the filler on the polymer properties. To our knowledge, this is the first time nanotitania doped with 1% Mn has been used as a nanofiller. This work is of significant importance to academia and industrial sectors due to its potential applications.

This proposal has the following main objectives:

1. To synthesize a novel nanocomposite composed of ethylene with nanotitania doped with 1% Mn using catalyst.
2. To compare the microstructure of polymers obtained by metallocene catalyst without fillers.
3. To study the effect of nanotitania on the polymer nanocomposite.
4. To study the properties of the nanocomposite.
5. To study the effects of the optimization parameters such as dosage of nanotitania, reaction time, reaction temperature, reaction pressure on the polymerization reactions.
6. Propose methodology to implement/apply the outcomes (results and recommendations) of the study.

Chapter 4

Experimental Methods

4.1 Materials

All manipulations were carried out under N₂ using standard Schlenk and glove box techniques. Titanium (IV) oxide containing 1% Mn as dopant, nanopowder (TiO₂/Mn), Cp₂ZrCl₂ and all other chemicals were purchased from Aldrich Chemicals and used without further purification. TiCl₄ activated with tri-isobutyl aluminum was used.

4.2 Characterization

Scanning electron microscope (SEM) was taken by HITACHI S-4200. Transmission electron microscope images were taken by JEOL, JEM 2011 (for high resolution TEM) and HITACHI H-7600. Molecular weight of PE were determined by High Temperature-Gel Permeation Chromatography using a light scattering detector in 1,2,4-trichlorobenzene. ¹H-NMR spectra of PE was taken in C₆H₄Cl₂ at 135 °C on Varian Unity Plus (300 MHz) spectrometer. The branching numbers for PE were determined by ¹H NMR spectroscopy using the ratio of number of methyl groups to overall number of carbons and were reported as branches per thousand carbons.

$$\text{Branches/ 1000 C} = \frac{\text{CH}_3 \text{ integral}}{\text{Total integral}} \times \frac{2}{3} \times 1000$$

4.2.1 Thermal analysis of the samples

The literature highlights the crystallinity having a relative influence on the mechanical properties of composites, therefore thermal analysis were carried out using DSC and TGA.

The thermal transition of the composites was evaluated using non-isothermal DSC analysis. The analysis was performed by using TA Q1000 instrument equipped with liquid nitrogen cooling system and auto sampler. The samples (sample size was around 6mg) in non- hermetic pan were heated at 10°C/min and cooled at the rate 5°C/min, and the temperature range of 20-170°C. The measurement process was as follows: first the sample was heated to 170°C, stayed for 5 minutes to eliminate the thermal history and then was cooled to observe the crystallinity behavior.

The thermal stability of the nanocomposites was studied using thermogravimetric analysis (TGA). TGA measurements were carried out using TA Instrument Hi-Res SDT Q600 thermogravimetric analyzer from 25 to 800°C with the heating rate of 10°C/min and a nitrogen gas flow rate of 50 cm³/min.

4.2.2 CRYSTAF

Crystallinity analysis of PE were determined by temperature rising elution fractionation (TREF) analysis (Polymer Char, Spain) using a light scattering detector in 1,2,4-trichlorobenzene. Crystallization is carried out in stainless-steel stirred vessels of 50-ml volume. Five crystallization vessels are installed in the main oven (a gas chromatography oven) and attached via a rotary valve to a dual-channel optoelectronic IR detector (with

3.5 μm as the measurement wavelength). Typical crystallization rates are 0.1–0.4°C/min.

The IR cell is kept heated isothermally during the whole experiment, typically at 150 °C.

4.3 Polymerization

4.3.1 Synthesis of PE-Doped TiO₂ Nanocomposites at low pressure

Ethylene polymerizations were performed in a 250 mL round-bottom flask equipped with a magnetic stirrer and a thermometer. The catalyst and required amount of TiO₂/Mn were added to the flask and the reactor was charged with toluene (80 mL). The reactor was immersed in a constant temperature bath previously set to desired temperature. When the reactor temperature had been equilibrated to the bath temperature, ethylene was introduced into the reactor after removing nitrogen gas under vacuum. When no more absorption of ethylene into toluene was observed, the cocatalyst was injected into the reactor and then the polymerization was started. Polymerization was quenched by the addition of methanol containing HCl (5 vol.-%) and then the unreacted monomer was vented. The polymer was washed with an excess amount of methanol and dried in vacuum at 50°C. To make a worthy comparison all data were collected under similar conditions.

4.3.2 Synthesis of PE-Doped TiO₂ Nanocomposites at High pressure

The polymerization was carried out in a 1-liter Autoclave reactor operated in a semi-batch mode. The reactor was carefully cleaned and dried under vacuum at 150°C for 3 hours,

and allowed to cool under nitrogen. Purified toluene was transferred to the reactor under nitrogen pressure through a transfer needle. The mixture was kept under stirring while the reactor was heated up to the desired polymerization temperature. Once the desired temperature was established, a prescribed amount of catalyst, co-catalyst and filler solution or slurry was added to the reactor under pure nitrogen atmosphere using gas-tight syringes. To start polymerization, the reactor was pressurized by ethylene to the desired pressure. The reactor was kept at constant pressure by continuous feeding of gaseous ethylene to the reactor. The reactor temperature was maintained within $\pm 1^{\circ}\text{C}$ of desired temperature by cooling circulation. The reaction was stopped by rapid depressurization of the reactor followed by quenching with methanol. The polymer was washed with an excess amount of methanol and dried in vacuum at 50°C . To make a worthy comparison all data were collected under similar conditions.

Chapter 5

Results and Discussion

5.1 Effect of Filler Concentration on the activity of the catalyst and polymer properties

It has been reported previously that change of metal centre in the catalyst structure can have remarkable effects on polymer structure and catalyst activity [63]. One of the main objectives of this work is to study the effect of doped nano titania on the activity of Cp_2ZrCl_2 & Cp_2TiCl_2 and polymer properties. The polyethylene nanocomposites were synthesized by in-situ polymerization using nanofillers. Table 5-1 shows the results of the polymerization runs carried out using the two catalyst and polymer properties. In this table, we have summarized the activity and other polymer properties by varying the filler concentration and we tried to investigate the effect of doped titania when compared to pure titania and manganese.

The increase in the concentration of nanofillers from 10 mg to 20 mg showed a distinct trend. The maximum polymerization activity was obtained using a filler concentration of 15 mg which was 431×10^3 gPE/mol Zr h bar. An increase in the filler concentration to 20 mg resulted in a decrease in the activity when compared to the 15 mg of filler concentration but still there is an increase in activity compared to the control. Thus there

is a significant increase in the catalytic activity in the presence of doped nanotitania with the concentration of 15 mg.

As shown in Table 5-1, nanotitanium oxide doped with manganese acted as the promoter in the polymerization process. To further understand the role of doped nanotitania, experiments were carried out with both pure titania and manganese. The optimum loading of 15 mg was used for both the runs.

Both the runs showed a marked decrease in the polymerization activity compared to nanotitanium oxide doped with manganese (15 mg filler incorporated) under the same reaction conditions. Thus confirming titanium doped with manganese plays a vital role in the polymerization reaction by enhancing the activity of the catalyst. This was likely due to interaction between MAO and TiO_2 [64].

It's a known fact that zirconocene has better activity compared to titanocene catalyst [65-66]. By taking this fact into consideration, we have tested the effect of filler at optimal concentration (15 mg) on the activity of titanocene catalyst. Similar to zirconocene, there is an increase in the catalytic activity of titanocene as well, which further shows that the doped nano titania acts as promoter even when we change the metal centre in the metallocene catalyst.

Table 5-1: Experimental conditions and properties of polyethylene prepared by insitu polymerization using Cp_2ZrCl_2 & Cp_2TiCl_2 catalyst and Methyl aluminoxane co-catalyst system.

Entry No.	Catalyst/Filler ^a (in mg)	Temp. (°C)	Time (minutes)	Activity ^e	Mn (g/mol)
1	A/0 ^b	30	30	152	9284
2	A/10	30	30	181	10900
3	A/15	30	30	431	4712
4	A/20	30	30	171	n.d ^f
5	A/15 ^c	30	30	121	11679
6	A/15 ^d	30	30	153	12817
8	A/15	30	60	364	10399
7	A/15	30	120	328	n.d
8	B/0	30	30	76	n.d
9	B/15	30	30	155	n.d

^a TiO_2 doped with Mn, ^b Control, ^c Pure TiO_2 , ^d Pure Mn, ^e $\times 10^{-3}$ gPE/mol h bar,

^f not determined, Catalyst (A = Cp_2ZrCl_2 , B = Cp_2TiCl_2)

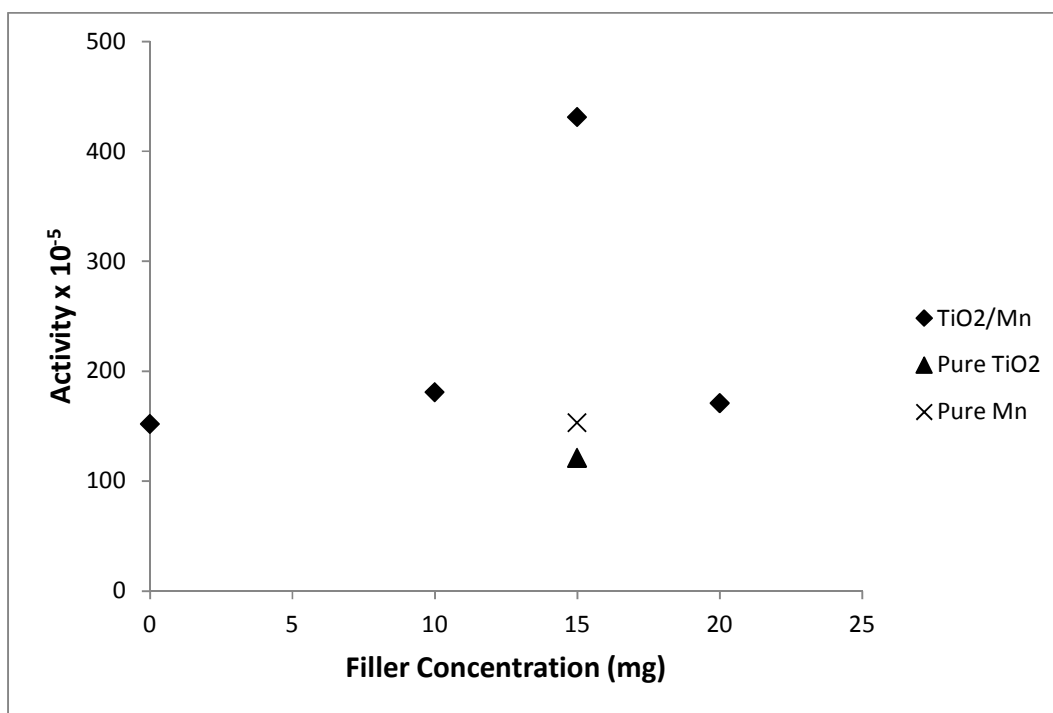
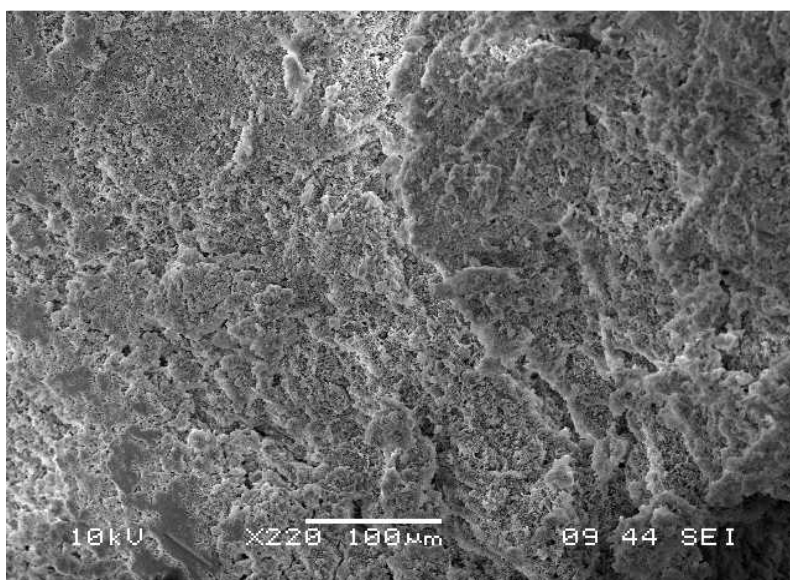


Figure 5-1: Activity of synthesized polyethylene nanocomposites using polymerization time of 30 mins at 30°C at 1 bar ethylene pressure

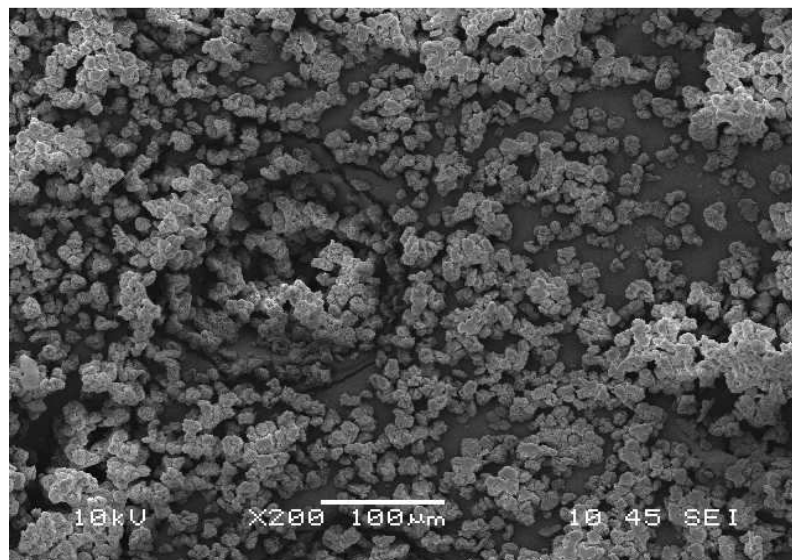
There is a remarkable effect of the filler on the molecular weight of the polymer. Though there is a steep increase in the catalytic activity by incorporating 15 mg of filler into the polymer system, there is also a decrease in the molecular weight of the polymer when compared with the other polymerization runs, which will in turn affect the thermal stability of the polyethylene nanocomposites. We could also find that there is increase in molecular weight of the polyethylene nanocomposite with respect to time. The thermal properties of these nanocomposites are discussed in detail in the next chapter.

In this course of study, we also have analyzed the impact of polymerization time on the catalytic activity. From Table 5-1, its clear that there is a decrease in the catalytic activity with respect to time, which is due to the deactivation of active sites.

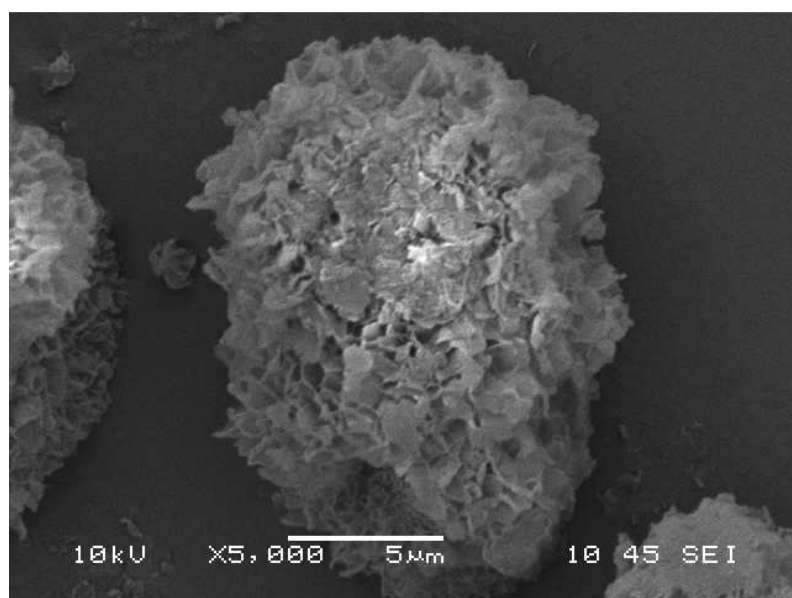
The doped-TiO₂/PE nanocomposites were further characterized by SEM and TEM to provide further insight into the polymerization process and nanocomposite properties. Figure 5-2a represents the SEM micrograph of the control i.e polyethylene without any nanofiller loading (Entry 1, Table1). Figure 5-2b shows the SEM micrograph of polyethylene synthesized using 15 mg TiO₂ doped with Mn (Entry 3, Table1) while Figure 5-2c shows a closer look at a single particle at a different magnification (Entry 3, Table1). Figure 5-2d presents the progressive growth of polyethylene synthesized with a polymerization time of 2 h (Entry 8, Table1). The micrographs clearly show the growth of the polymer while also showing a good dispersion. It indicates that the doped-TiO₂ nanoparticles have a nucleus effect on the polymerization and caused a homogeneous PE shell around them. The SEM images help us to draw a conclusion that the doped TiO₂ has a strong effect on the PE's morphology and with the increase in polymerization time, the composites show a growth in its particle size which symbolizes that the catalyst was active even after long time.



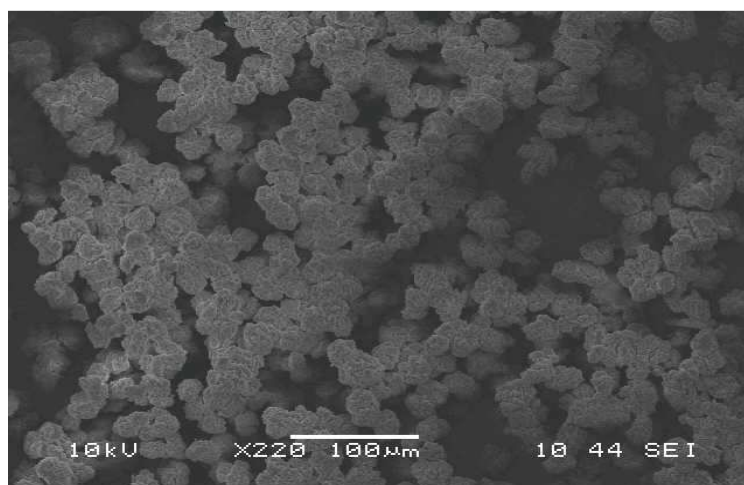
(a)



(b)



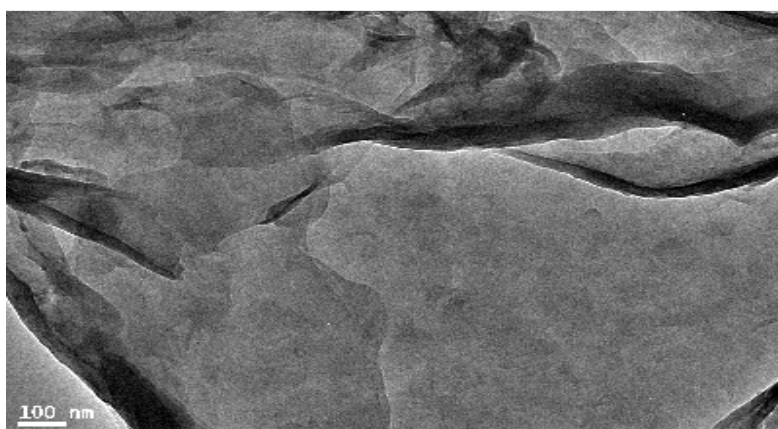
(c)



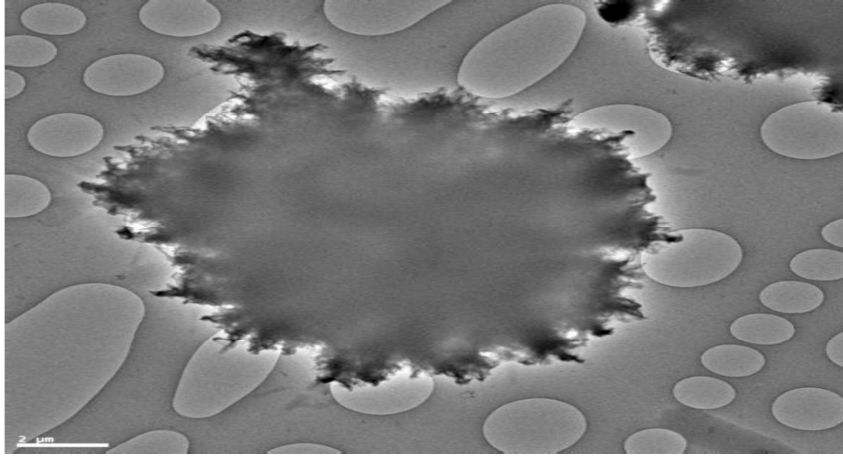
(d)

Figure 5-2: SEM micrographs of (a) Control (Entry 1, Table1) (b) Polyethylene with 15 mg of TiO_2/Mn using polymerization time of 30 mins (Entry 3, Table1) (c) Higher magnification of polyethylene with 15 mg of TiO_2/Mn using polymerization time of 30 mins (Entry 3, Table1) (d) Polyethylene prepared using polymerization time of 120 mins (Entry 8, Table1).

On comparing the TEM images Figure 5-3a represents the TEM micrograph of the control i.e polyethylene without any nanofiller loading. Figure 5-3b shows the TEM micrograph of polyethylene synthesized using TiO_2 doped with Mn, representative for the overall material; it is evident from these micrographs that a PE layer, whose thickness increases with time, thus filler is uniformly embedded into the polyethylene matrix.



(a)



(b)

Figure 5-3: TEM micrographs of (a) Control (Entry 1, Table1) (b) Polyethylene with 15 mg of TiO₂/Mn (Entry 3, Table1)

The dispersion of filler in the polymer matrix is very important in enhancing the properties of the polymer nanocomposites. The improvement of doped-TiO₂ dispersion in PE matrix can be visibly checked by WAXD. Figure 5-4 shows the WAXD patterns of doped-TiO₂, Control, and PE/ doped-TiO₂ nanocomposites. The doped-TiO₂ has a sharp Bragg reflection at about $2\theta=27^\circ$. WAXD curves of PE/ doped-TiO₂ nanocomposites show disappearance of the basal peak, indicating that doped-TiO₂ is well dispersed in PE matrix during polymerization [67]. The strong reflections observed for the control were also present for comparison. This figure shows that the addition of doped-TiO₂ does not change the original crystal structure.

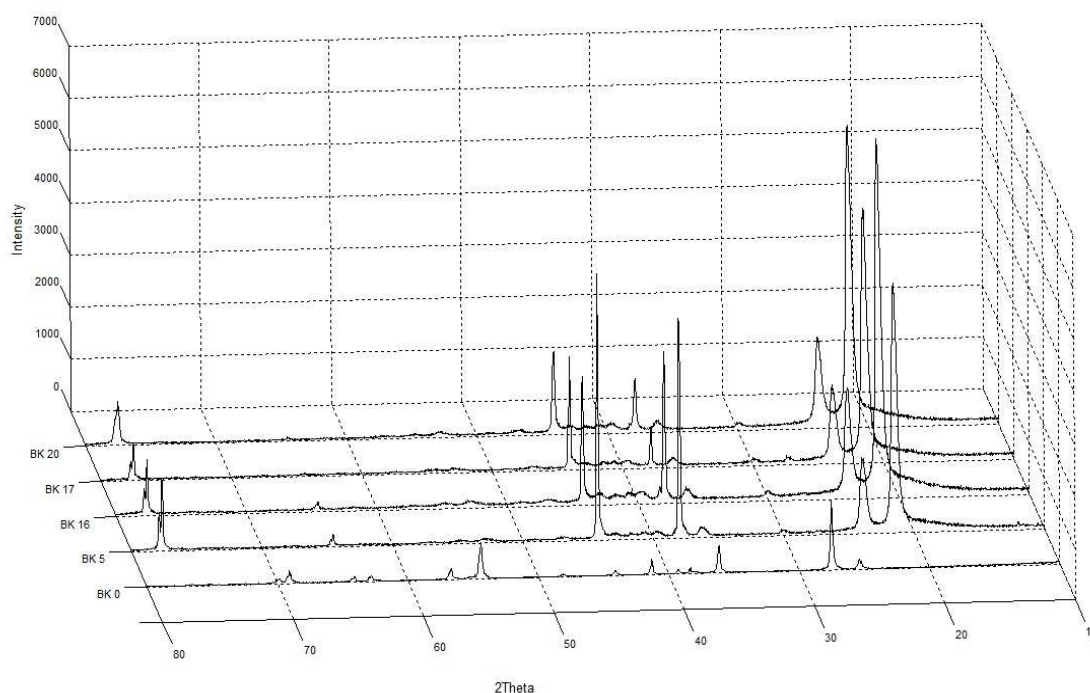


Figure 5-4: WAXD patterns of doped-TiO₂ (BK 0), Control (BK 20), and PE/doped-TiO₂ nanocomposites (BK 16, BK 17 & BK 5)

5.2 Effect of Polymerization Conditions on Catalyst Activity and Polymer Properties

The effects of reaction temperature and ethylene pressure on catalyst activity were very clear from the experimental data. There was an increase in activity of zirconocene in the presence of filler at 30°C of polymerization temperature, but activity got decreased at higher temperature. This temperature effect on activity was observed by maintaining the ethylene pressure at 1 bar and by varying reaction temperature as shown in Table 5-2

Table 5-2: Experimental conditions and properties of polyethylene prepared by insitu polymerization using Cp_2ZrCl_2 & Cp_2TiCl_2 catalyst and Methyl aluminoxane co-catalyst system.

Entry No.	Catalyst/Filler ^a (in mg)	Temp. (°C)	Time (minutes)	Activity ^c
1	A/0 ^b	30	30	152
2	A/15	30	30	431
3	A/0	60	30	281
4	A/15	60	30	255
5	B/0	30	30	76
6	B/15	30	30	155
7	B/0	60	30	141
8	B/15	60	30	115

^a TiO_2 doped with Mn, ^b Control, ^c $\times 10^{-3}$ gPE/mol h bar, Catalyst (A = Cp_2ZrCl_2 , B = Cp_2TiCl_2)

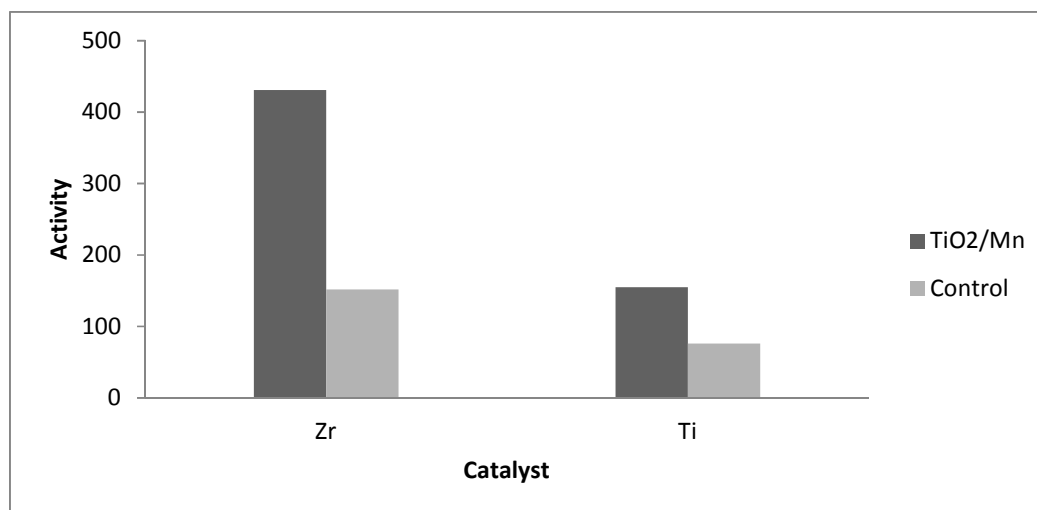


Figure 5-5: Polymerization activity of metallocene (Zr - Cp_2ZrCl_2 , Ti - Cp_2TiCl_2) to form polyethylene nanocomposites (Temperature-30°C, Time-30 mins, and Ethylene pressure-1 bar)

From Figure 5-6, it is evident that there is an increase in the catalytic activity with the increase in the polymerization temperature in the absence of filler, this phenomenon is due to the increase in the chain propagation rate which will in turn increase the activity of the catalyst. Though there is an increase in the catalytic activity at 60°C in the absence of filler (281×10^3 gPE/mol Zr h bar), this increase is not as high as at 30°C in the presence of filler (431×10^3 gPE/mol h bar). A similar trend was found even with titanocene catalyst. The activity is high in the presence of filler at 30oC (155×10^3 gPE/mol h bar) compared to control even at 60°C (141×10^3 gPE/mol h bar), this point is discussed in detail with the help of Figure 5-7 and Figure 5-8.

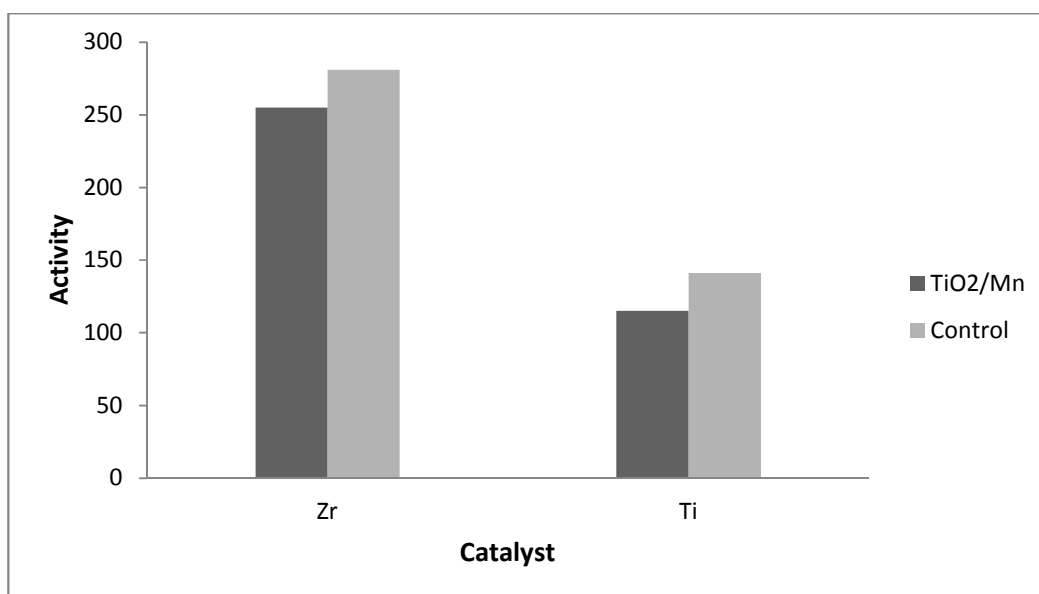


Figure 5-6: Polymerization activity of metallocene (Zr - Cp_2ZrCl_2 , Ti - Cp_2TiCl_2) to form polyethylene nanocomposites (Temperature-60°C, Time-30 mins, and Ethylene pressure-1 bar)

From the Figure 5-7, we are able to infer that the activity of the catalyst decreases with the increase of the reaction temperature in presence of filler. The low yield as a result of

the filler addition could be due to more steric hindrance arising from the nanoparticles and strong interaction might have happened between the filler and the co-catalyst [68].

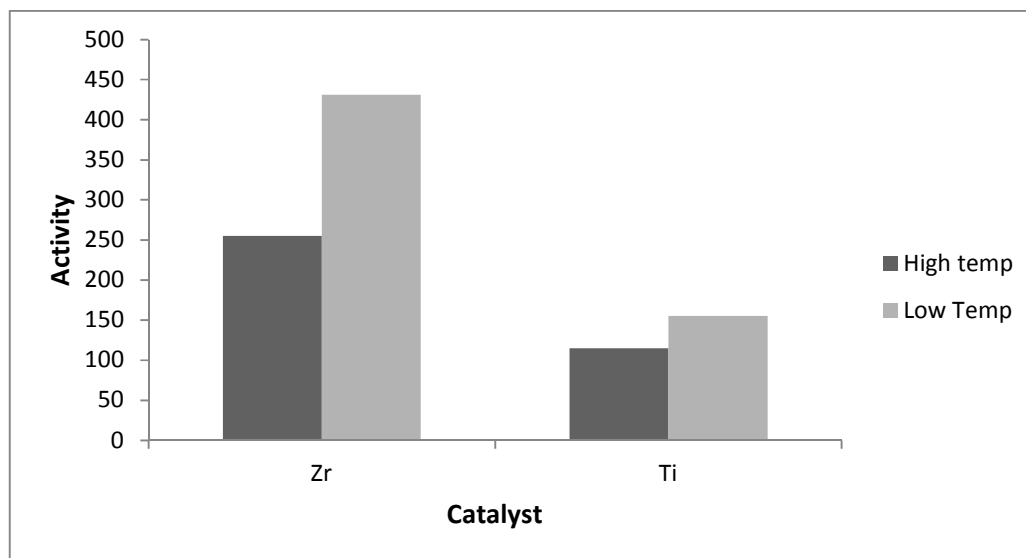


Figure 5-7: Polymerization activity of metallocene (Zr - Cp_2ZrCl_2 , Ti - Cp_2TiCl_2) to form polyethylene nanocomposites (Temperature-30°C & 60°C, Time-30 mins, and Ethylene pressure-1 bar)

From Figure 5-8, its quiet obvious that in the case of both the catalyst, the activity is high in the presence of filler at 30°C, thus as far as the current experimental results this sounds to be the ideal condition for proceeding further with the synthesis of these kinds of nanocomposites.

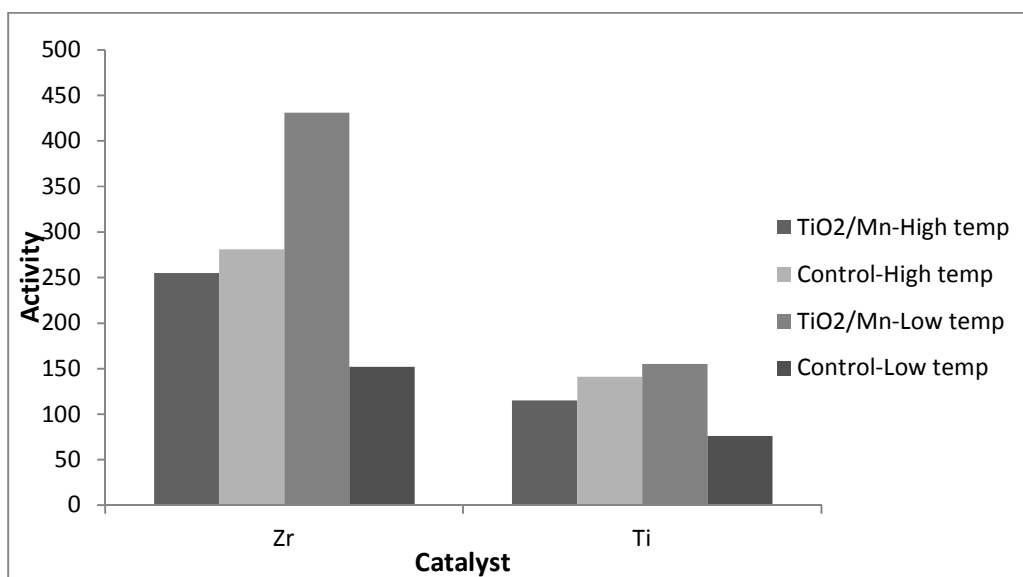


Figure 5-8: Effect of temperature on the polymerization activity of the metallocene(Zr - Cp_2ZrCl_2 , Ti - Cp_2TiCl_2) to form polyethylene nanocomposites (Time-30 mins, Ethylene pressure – 1 bar)

As for the effect of high pressure on the catalytic activity, the trend is much similar to the catalytic activity at low pressure. Table 5-3 presents the experimental data with respect to increase in the ethylene pressure and by maintaining the reaction temperature at 30°C. The trend in the catalytic activity of zirconocene catalyst shows the increase in catalytic activity with ethylene pressure, this is due to the fact that the catalytic active sites are exposed to more ethylene at high pressure.

Table 5-3: Experimental conditions and properties of polyethylene prepared by insitu polymerization using Cp_2ZrCl_2 catalyst and Methyl aluminoxane co-catalyst system.

Entry No.	Filler ^a	Pressure	Temp.	Time	Activity ^b
	(in mg)	(bar)	(°C)	(minutes)	
1	0	5	30	30	156
2	15	5	30	30	496
3	15	5	30	60	454
4	15	5	30	120	404
5	15	2	30	30	266

^a TiO_2 doped with Mn, ^b $\times 10^{-3}$ gPE/mol h bar,

From Figure 5-9, it is clear that the activity of the catalyst in presence of filler is more at pressure of 2 bar compared to the activity of the catalyst in absence of filler even at much higher pressure, this illustrates the role of filler as promoter in the polymerization process also at different pressures.

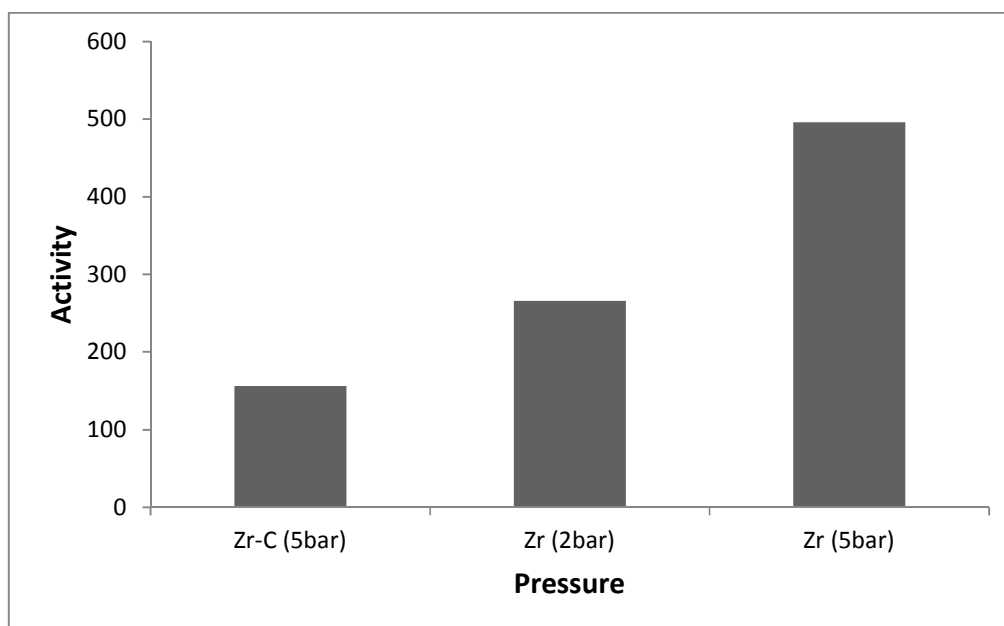


Figure 5-9: Effect of pressure on the activity of the catalyst ($\text{Zr} - \text{Cp}_2\text{ZrCl}_2$), here Zr-C represents the Control and other two represents the nanocomposites with filler at 30°C with reaction time of 30 mins

We have also tested the effect of time on the catalytic activity and the properties of the polymer, which is illustrated in the better fashion through Figure 5-10. These experiments were carried out at constant pressure of 5 bar and at polymerization temperature of 30°C . In which we can see there is a uniform decrease in the catalytic activity with respect to time, this is due to the deactivation of active sites. Their impact on the thermal and mechanical properties of the polyethylene is studied in detail in the next chapter.

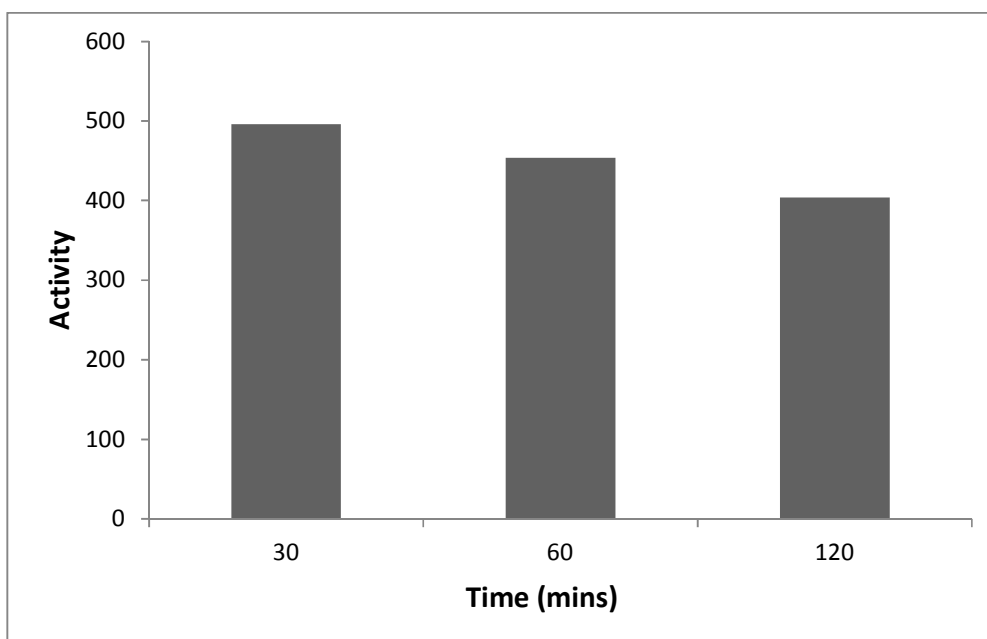


Figure 5-10: Effect of time on the activity of the catalyst($\text{Zr} - \text{Cp}_2\text{ZrCl}_2$) with reaction time of 30 mins at 30°C at 5 bat ethylene pressure.

5.3 Effect of Filler concentration & Polymerization time on the thermal properties of polymer

Thermal properties of Polyethylene/doped-TiO₂ nanocomposites are reported in Table 5-4. A strong correlation was observed between filler loading and the degree of branching in polymer produced as evident in the DSC thermal analysis. We reported the DSC thermal analysis in terms of melting temperature (T_m) and degree of crystallinity (X_c). The melting behavior of polyethylene is mainly related to the short chain branching density.

Increasing short chain branching density decreases lamellar thickness of the crystal structure and thus lowers melting temperature of the polymer. The short chain branching also affects the degree of crystallinity which is proportional to the fractional amount of crystalline phase in polymer sample [69].

It can be observed from Table 5-4 that at the optimal concentration of filler loading (15 mg) there is a slight decrease in melting temperature compared to the control though there isn't much difference in the degree of short chain branching which symbolize that the promoter effect of filler doesn't affect the thermal property to a great extent. But when the filler concentration is equal to 10 mg there is decrease in the melting temperature which corresponds to the increase in the degree of short chain branching which is the case even when we increase the filler concentration to 20 mg. By comparing the doped-titania with the pure titania and manganese, we found that there is a slight increase in the degree of short chain branching which has an impact in the crystallization percentage of these nanocomposites. Figure 5-11-5-12 represents the second heating curve obtained from DSC analysis.

Table 5-4: Experimental conditions and properties of polyethylene prepared by insitu polymerization using Cp_2ZrCl_2 & Cp_2TiCl_2 catalyst and Methyl aluminoxane co-catalyst system.

Entry No.	Catalyst/Filler ^a (in mg)	Temp. (°C)	Time (minutes)	T _m ^e (°C)	Xc ^e (%)	Branches/1000 C ^f
1	A/0 ^b	30	30	133	78	5
2	A/10	30	30	131	76	9
3	A/15	30	30	130	80	5
4	A/20	30	30	131	74	8
5	A/15 ^c	30	30	135	76	7
6	A/15 ^d	30	30	134	73	6
7	A/15	30	60	131	75	n.d. ^g
7	A/15	30	120	132	75	8
8	B/0	30	30	134	78	3
9	B/15	30	30	135	58	7

^a TiO_2 doped with Mn, ^b Control, ^c Pure TiO_2 , ^d Pure Mn, ^e Determined by DSC measurements, ^f Determined by NMR analysis, Catalyst (A = Cp_2ZrCl_2 , B = Cp_2TiCl_2), ^g not determined

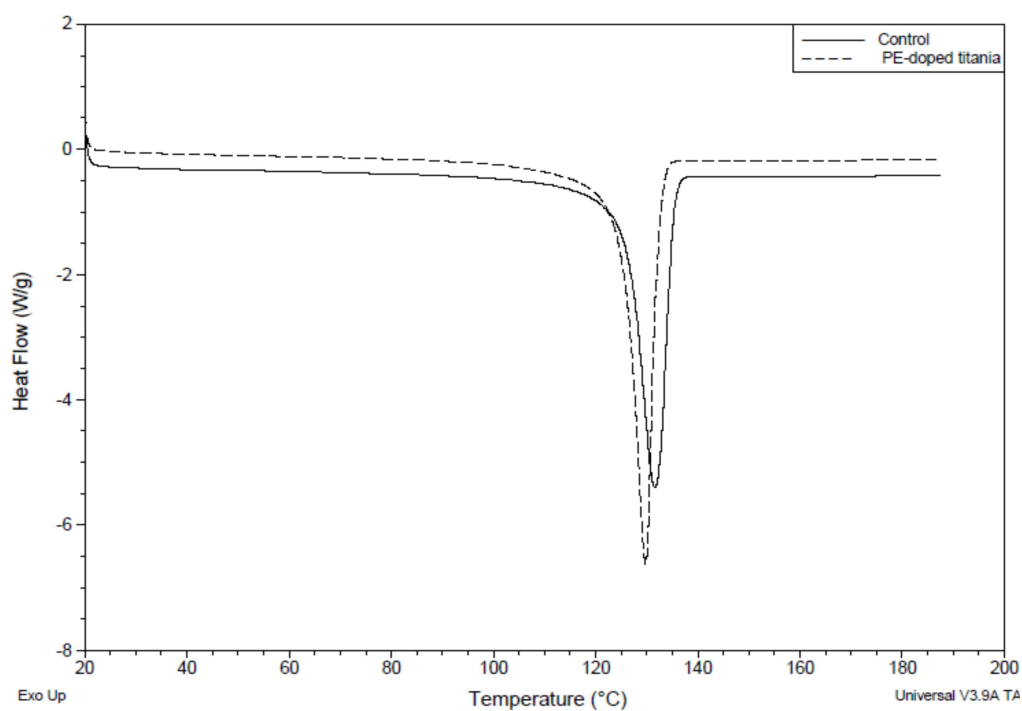


Figure 5-11: DSC second heating curves of homopolymer, polyethylene with doped-titania (15 mg) synthesized using Cp_2ZrCl_2 catalyst

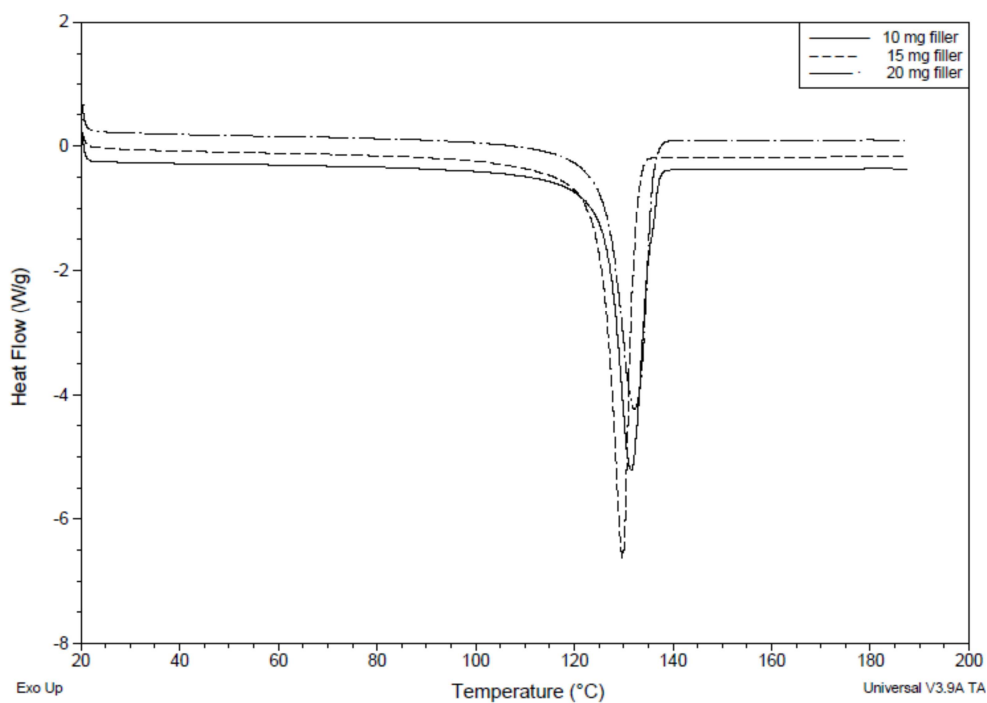


Figure 5-12: DSC second heating curves of polyethylene with doped-titania using different concentrations of filler with Cp_2ZrCl_2 catalyst

It can be observed from Table 1 that the crystallinity (X_c) of polyethylene increased at optimal filler concentration of 15 mg. This shows that the presence of small amounts of filler in PE/doped-TiO₂ nanocomposites will enhance the crystallinity of PE. This also indicates that the dispersed doped-TiO₂ particles act as nucleating agents for PE crystallization as it offers more sites for crystal growth in the matrix. But there is a slight decrease in the crystallinity of these nanocomposites when we move from the optimal concentration. As we can see from Table 5-4, the crystallinity at 10 mg and 20 mg are less compared to the control, this characteristic feature could indicate that the crystallization of PE is adversely affected by the close vicinity of the doped-TiO₂ surface since doped-TiO₂ could be considered as a good nucleating agent which was proven initially through SEM images. The crystallinity followed the same trend also in the case of pure titania and pure manganese, where there is a decrease in the crystallinity as like doped-TiO₂ at different concentrations.

Nanocomposite obtained from zirconocene showed lower branching (eg. 5 branches/1000 C) than that of from titanocene (eg. 7 branches/1000 C). The melting behavior of PE is mainly related to short chain branching density. An increase in short chain branching density decreases the lamellar thickness of crystal structure thereby lowers the melting temperature of polymer. Since there is an increase in the degree of short branching in the case of titanocene, we could find that there is a decrease in the crystallinity of the nanocomposites. Figure 5-13-5-15 represents the second heating curve obtained from DSC analysis.

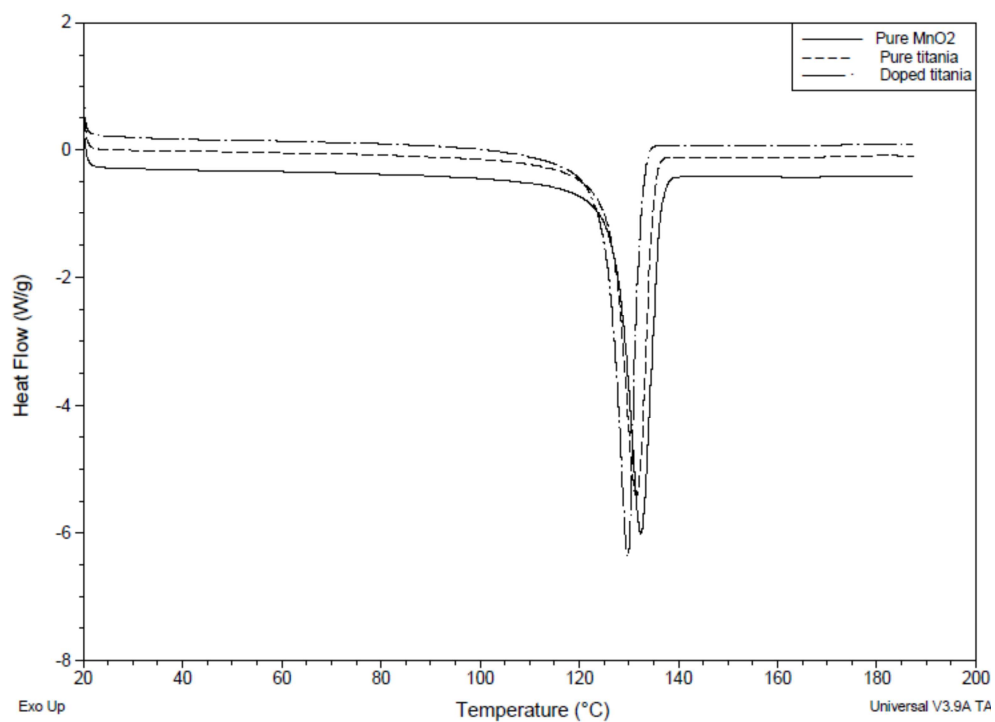


Figure 5-13: DSC second heating curves of polyethylene with different fillers with Cp_2ZrCl_2 catalyst

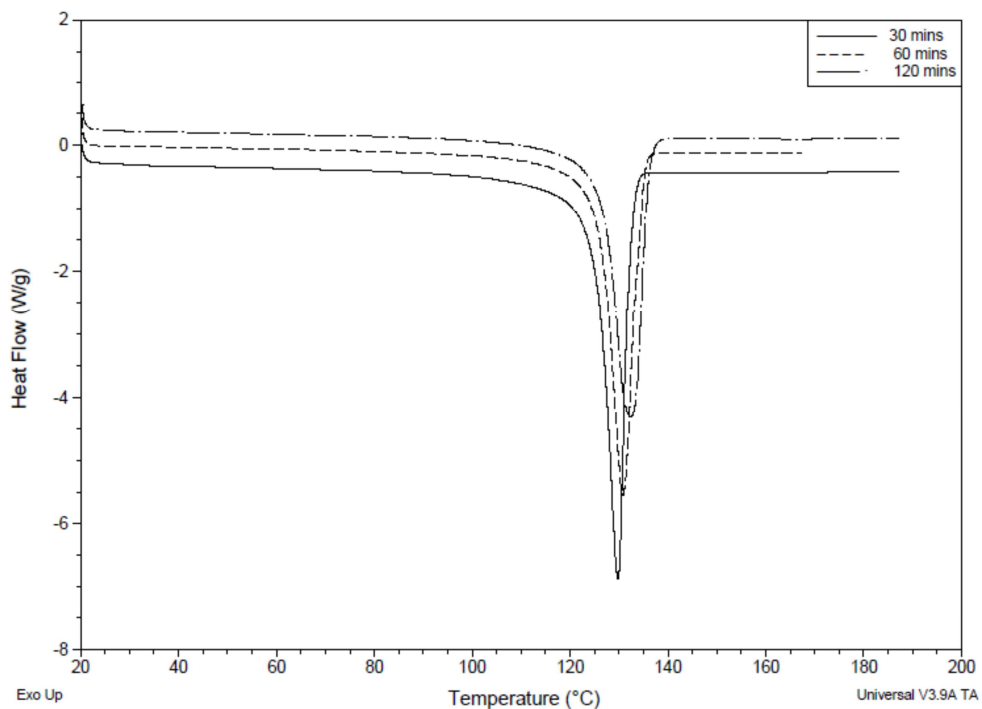


Figure 5-14: DSC second heating curves of polyethylene with different polymerization time with Cp_2ZrCl_2 catalyst

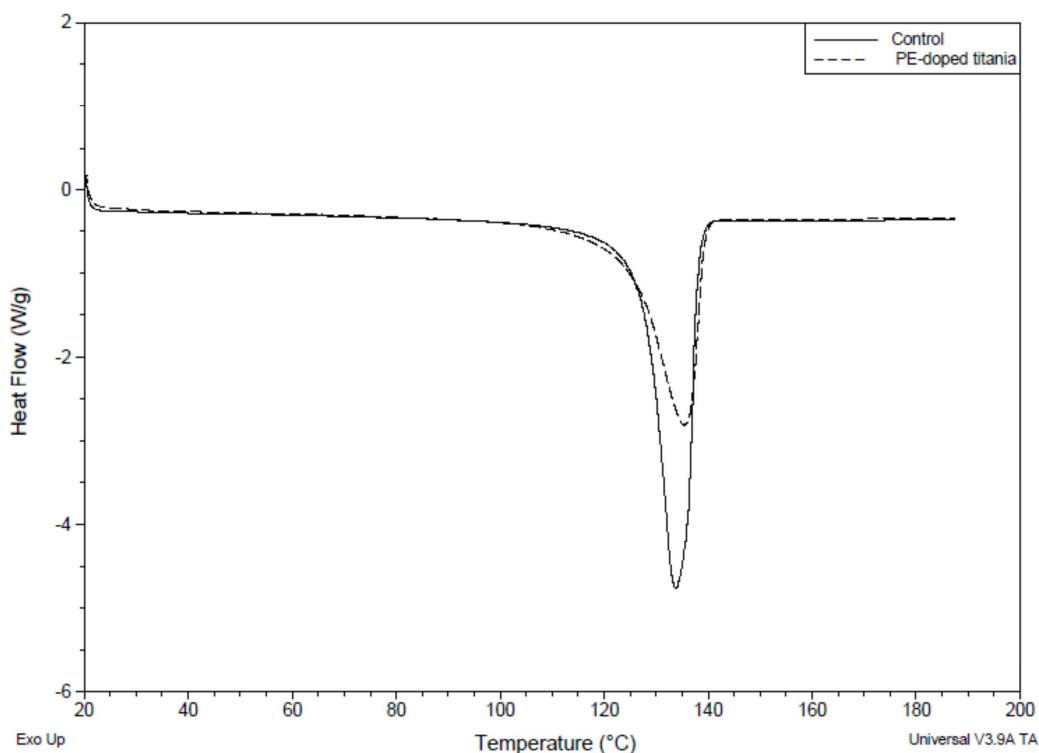


Figure 5-15: DSC second heating curves of homopolymer, polyethylene with doped-titania (15 mg) synthesized using Cp_2TiCl_2 catalyst

CRYSTAF analysis of the PE supported the above results. Those can be used to measure chemical composition distribution (CCD) based on the continuous crystallization of polymer chains from a dilute solution [70-73]. The knowledge of a polymer's CCD is essential in investigations of structure-property relationships, polymerization kinetics and mechanisms, and polymer reaction engineering [72]. CRYSTAF profiles for one polymer nanocomposite with the optimal concentration of filler and PE from control are shown in Figure 5-16. From the Figure 5-16, the crystallization peak temperatures are around 83°C for both homopolymer and nanocomposite respectively. From the Table 5-4 it is clear that branching frequency is 5 per 1000 backbone carbon for both the cases respectively. Generally the crystallization peak temperatures is inversely proportional to the degree of short chain branching.

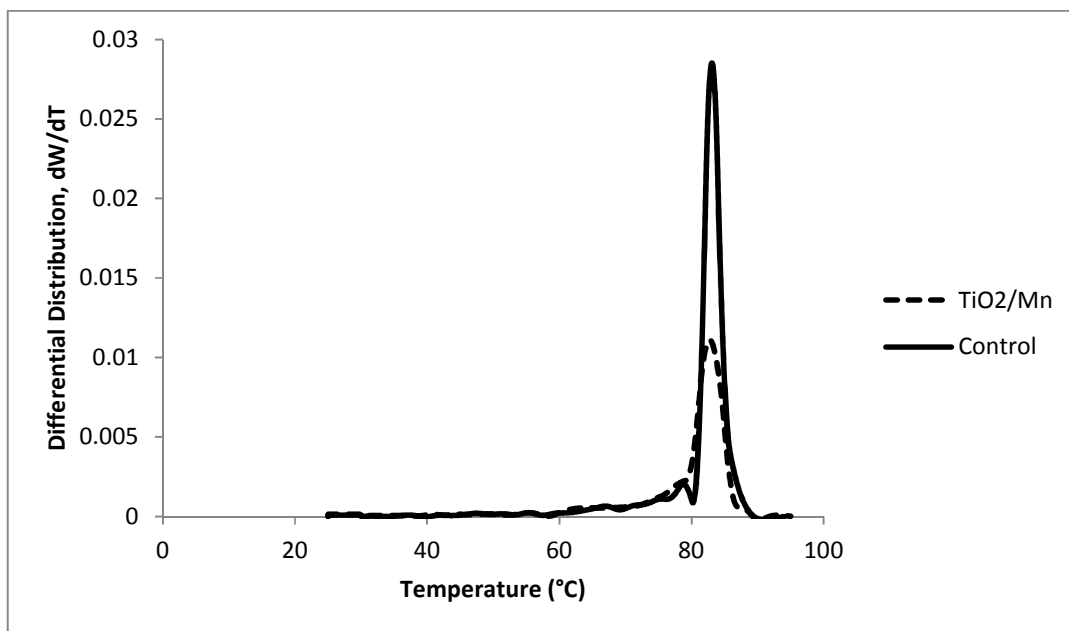


Figure 5-16: CRYSTAF analysis of polymer nanocomposite obtained by Cp_2ZrCl_2 catalyst; a) in the absence of doped-titania b) in the presence of doped-titania. (Temperature-30 $^{\circ}C$, Ethylene Pressure-1 bar, Time-30mins)

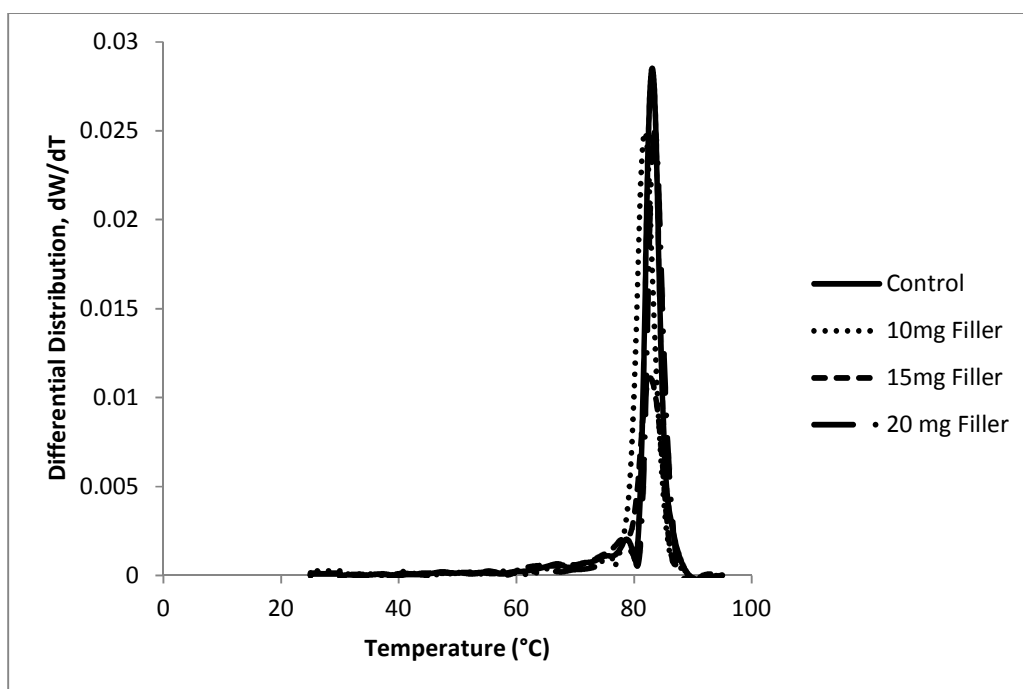


Figure 5-17: CRYSTAF analysis of polymer nanocomposite obtained by Cp_2ZrCl_2 catalyst at different concentrations of filler (Temperature-30 $^{\circ}C$, Ethylene Pressure-1 bar, Time-30mins)

Figure 5-17 corresponds to the CRYSTAF analysis plot of polyethylene nanocomposites synthesized at different concentrations of filler. From this we could infer that there is slight decrease in the crystallization temperature at 10 mg of filler which corresponds to increase in short chain branching. From Figure 5-18, we could find that there isn't much difference in the crystallinity temperature between the homopolymer and the nanocomposite.

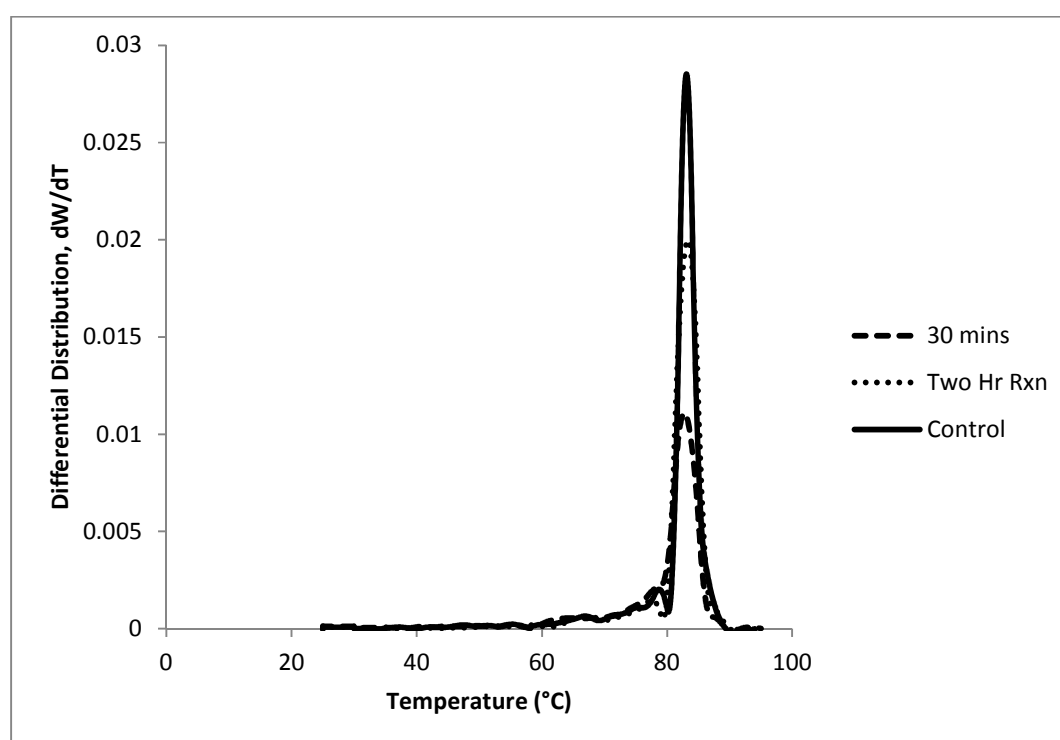


Figure 5-18: CRYSTAF analysis of polymer nanocomposite obtained by Cp_2ZrCl_2 catalyst at optimal concentration of filler by varying the reaction time (Filler concentration-15 mg, Temperature-30°C, Pressure-1 bar)

In case of TGA curves which are shown in the below figures, thermal stabilization of all the nanocomposites and the fraction of volatile components are observed under inert nitrogen atmosphere.

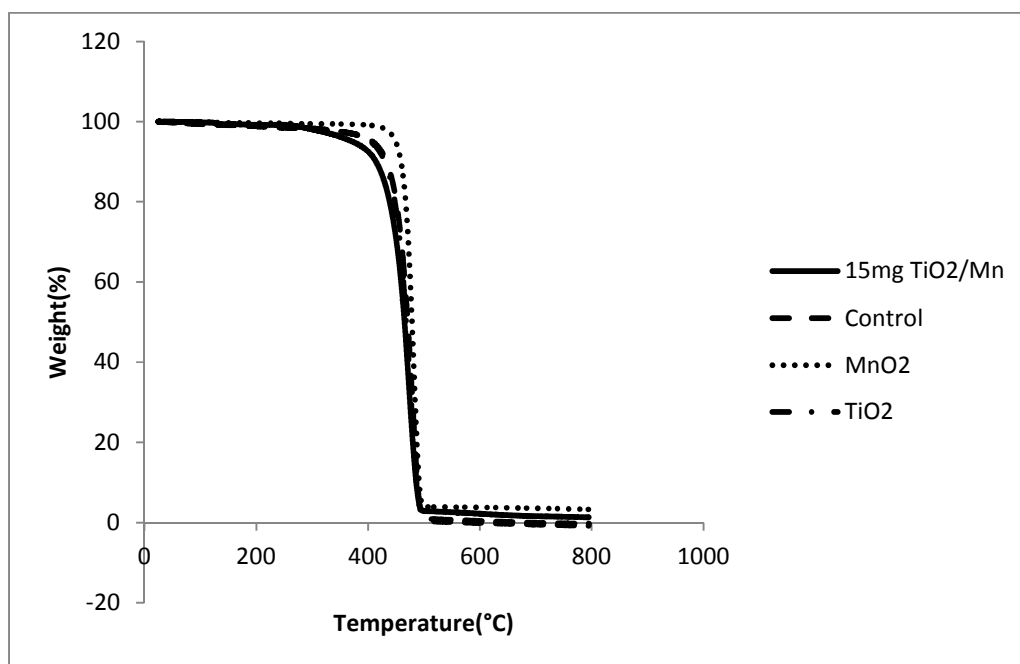


Figure 5-19: TGA curves of homopolymer, polyethylene with doped-titania, polyethylene with pure titania and polyethylene with pure manganese oxide synthesized using Zirconocene catalyst

From the Figure 5-19, it is clear that the thermal stability of polyethylene nanocomposite with doped-titania is comparatively less than the homopolymer, this is due the difference in their molecular weight. As we discussed in previous chapter, the molecular weight of polyethylene/doped-titania nanocomposite is less than the homopolymer. From the above Figure, its also clear that the polyethylene nanocomposite with pure manganese have high thermal stability compared to the polyethylene nanocomposite with pure titania and doped titania. When we analyze the ash content, which is the amount of metal catalyst in the material. It is usually assumed that upon completion of TGA, all carbon has been removed in the forms of CO and CO₂ and that all remaining material consists of metal oxides. In the case of polyethylene/doped-titania nanocomposite less ash is found which is due to the polymer to filler ratio, since the activity in the presence of doped-titania is

very high, the filler weight percentage is very low which corresponds to less ash content in the TGA curves.

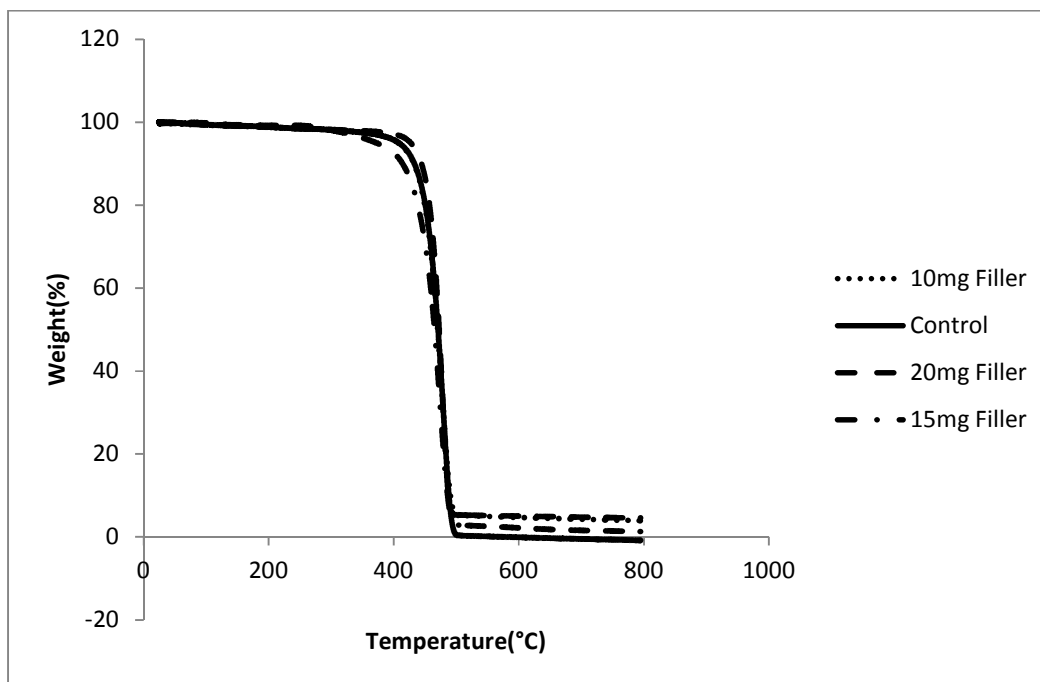


Figure 5-20: TGA curves of homopolymer and polyethylene with doped-titania at different filler concentrations using Zirconocene catalyst

From Figure 5-20, its very apparent that the thermal stability of polyethylene/doped-titania nanocomposite at optimal concentration of 15 mg is low compared to other two concentration. But the interesting fact which we can conclude from this figure is that there is an increase in thermal stability of the polyethylene when the concentration is 20 mg, but at this stage we could find more ash is left out which is due to the filler weight percentage. Since, in the case of 10 mg and 20 mg of filler concentration the activity of the catalyst was low, which corresponds to more filler weight percentage in these nanocomposites compared to the filler weight percentage in the nanocomposite

synthesized at optimal concentration of 15 mg. The thermal stability of these nanocomposites corresponds to the molecular weight of each polymer, thus this proves that the molecular weight of polyethylene in presence of 15 mg of doped-titania is low compared to the molecular weight of polyethylene in presence of doped-titania in other two concentrations.

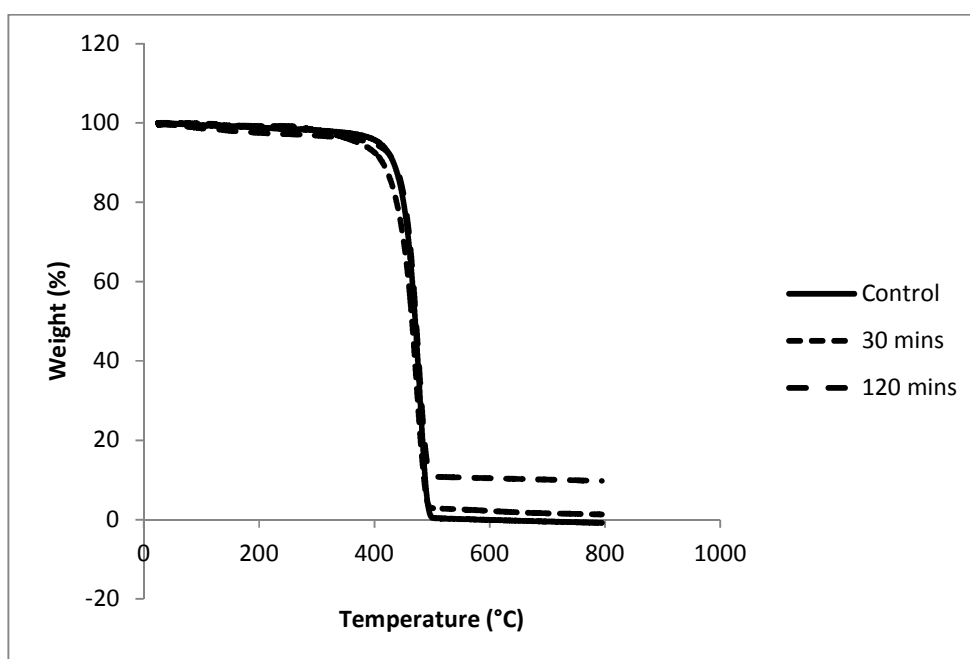


Figure 5-21: TGA curves of homopolymer and polyethylene with doped-titania synthesized by varying the reaction time using Zirconocene catalyst

From above figure, we can conclude that the thermal stability of the polyethylene nanocomposite increases with reaction time, which further helps us to infer that there is an increase in molecular weight of these nanocomposites with respect to time. In this figure, we could see that the ash content is more for the polyethylene nanocomposite synthesized using a reaction time of 30 mins compared to 2 h, which is due to the filler weight percentage in these nanocomposites.

From Figure 5-22, it is clear that by the change of metal centre in the metallocene the thermal stability is not much affect. Here we can find that the polyethylene in the absence of filler shows better thermal stability compared to the polyethylene nanocomposites which is due to the fact that there is a difference in the molecular weight of these synthesized polyethylene, the addition of filler lowers the molecular weight which in turn decreases the thermal stability of the polymer. When we analyse the ash content from the TGA curve, we could conclude that filler weight percentage plays the crucial role, because the ash content increases with the increase in filler weight percentage in the polyethylene nanocomposite which is vividly illustrated in the given figure.

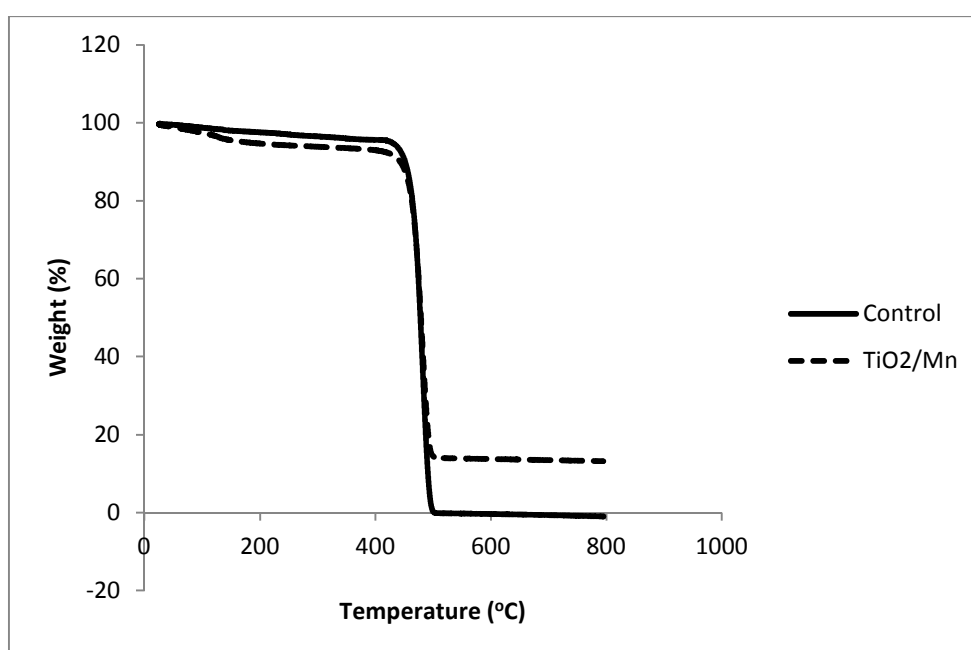


Figure 5-22: TGA curves of homopolymer and polyethylene with doped-titania synthesized using Titanocene catalyst

5.4 Effect of Polymerization Conditions on Thermal Properties of Polymer

The effects of reaction temperature and ethylene pressure on catalyst activity were very clear from the experimental data. There was a decrease in the melting temperature of Zirconocene in the presence of filler at 60°C of polymerization temperature due to the increase in degree of short of branching. This temperature effect on activity was observed by maintaining the ethylene pressure at 1 bar and by varying reaction temperature as shown in Table 5-5

Table 5-5: Experimental Conditions and properties of polyethylene prepared by insitu polymerization using Cp_2ZrCl_2 & Cp_2TiCl_2 catalyst and Methyl aluminoxane co-catalyst system.

Entry No.	Catalyst/Filler ^a	Temp.	Time	T _m ^c	Xc ^c	Branches/1000 C ^d
	(in mg)	(°C)	(minutes)	(°C)		
1	A/0 ^b	30	30	133	78	5
2	A/15	30	30	130	80	5
3	A/0	60	30	131	68	n.d ^f
4	A/15	60	30	125	74	11
5	B/0	30	30	134	78	3
6	B/15	30	30	135	58	7
7	B/0	60	30	134	69	n.d
8	B/15	60	30	134	61	n.d

^a TiO_2 doped with Mn, ^b Control, ^c Determined by DSC measurements, ^d Determined by NMR analysis, ^f not determined, Catalyst (A = Cp_2ZrCl_2 , B = Cp_2TiCl_2)

From Table 5-5, it is evident that the decrease in temperature increases the melting temperature in the case of Zirconocene in the presence of doped-titania, this trend showed a reduction in the short chain branch content due to the dominance of chain propagation over chain walking reactions at such conditions [69].

Nanocomposite obtained from zirconocene showed lower branching (eg. 5 branches/1000 C) than that of from titanocene (eg. 7 branches/1000 C). The melting behavior of PE is mainly related to short chain branching density. An increase in short chain branching density decreases the lamellar thickness of crystal structure thereby lowers the melting temperature of polymer. Since there is an increase in the degree of short branching in the case of titanocene, we could find that there is a decrease in the crystallinity of the nanocomposites. The same trend is being followed even at high temperature as we could see that the degree of crystallinity for titanocene is lower than the zirconocene which in turn relate to high degree of short chain branching.

In Figure 5-23, we could find that the polyethylene nanocomposite synthesized at high temperature shows a broad melting peak, this observation could be attributed to more irregularity of the chain structure of the polyethylene produced by zirconocene catalyst [69].

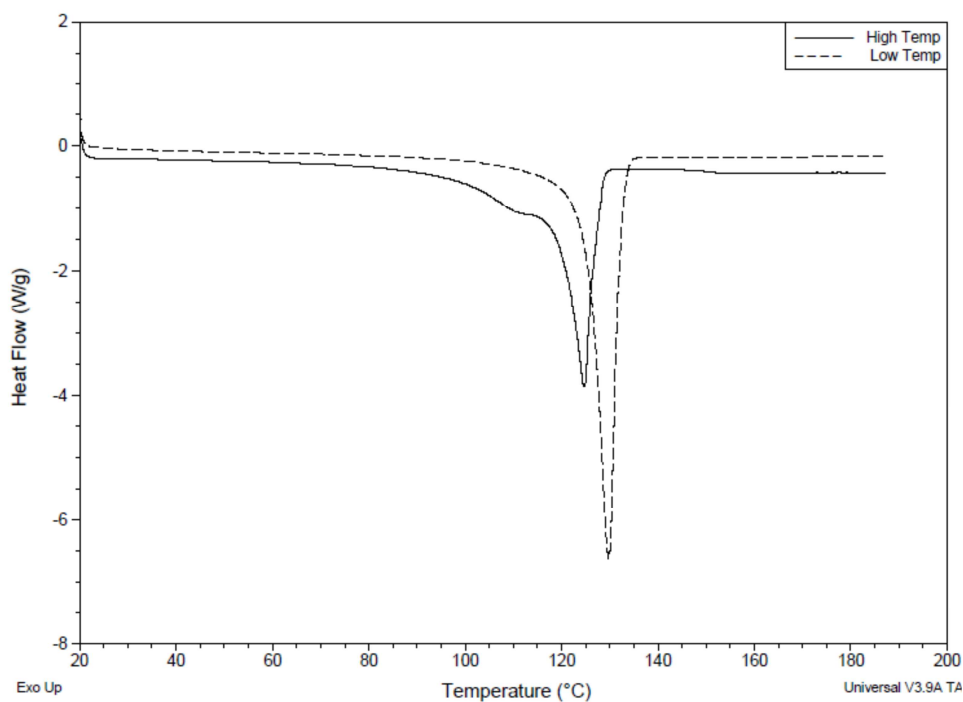


Figure 5-23: DSC second heating curves of homopolymer synthesized at high temperature, polyethylene with doped-titania synthesized at high temperature and low temperature using Zirconocene.

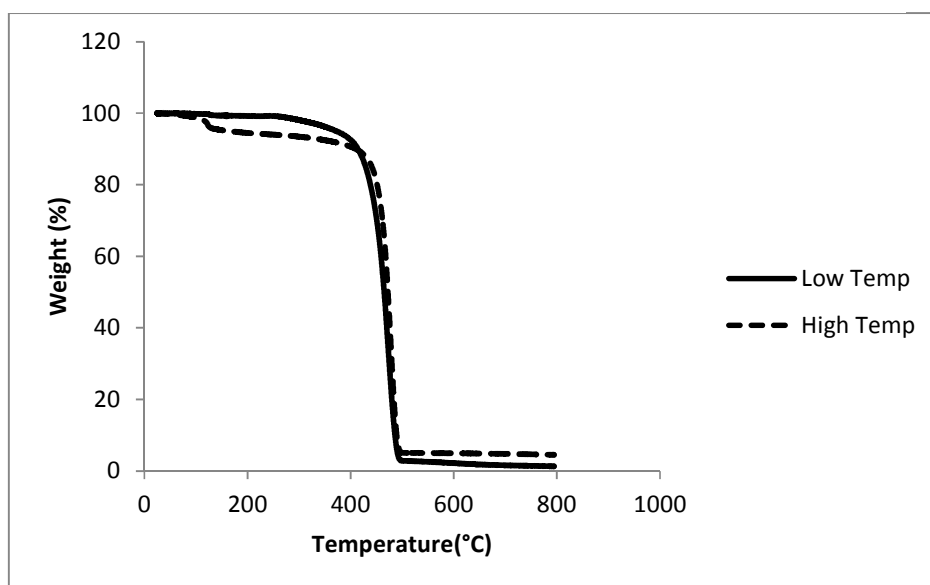


Figure 5-24: TGA curves of polyethylene with doped-titania synthesized at different polymerization temperatures using Zirconocene catalyst

From the TGA analysis of polyethylene nanocomposites we could infer that the thermal stability of polyethylene increases with the temperature as the degradation temperature of polyethylene nanocomposites synthesized at high temperature is 478°C, whereas the degradation temperature of polyethylene nanocomposites synthesized at low temperature is 474°C. This increase in the degradation temperature is due to the increase in the molecular weight of these sample, but it known that as the temperature increases further there will be decrease in the thermal stability due to the decrease in molecular weight which will show the predominance of chain transfer reaction at high temperature.

There is a difference in the ash content of these polyethylene nanocomposites which is due to the filler weight percentage. As we discussed in the previous chapter, the activity of the catalyst was low at high temperature which means less yield of polyethylene was obtained. The weight percentage of filler is more when the polyethylene nanocomposites are synthesized at high temperature thus it is reasonable to get more ash content for the polyethylene nanocomposites synthesized at high temperature.

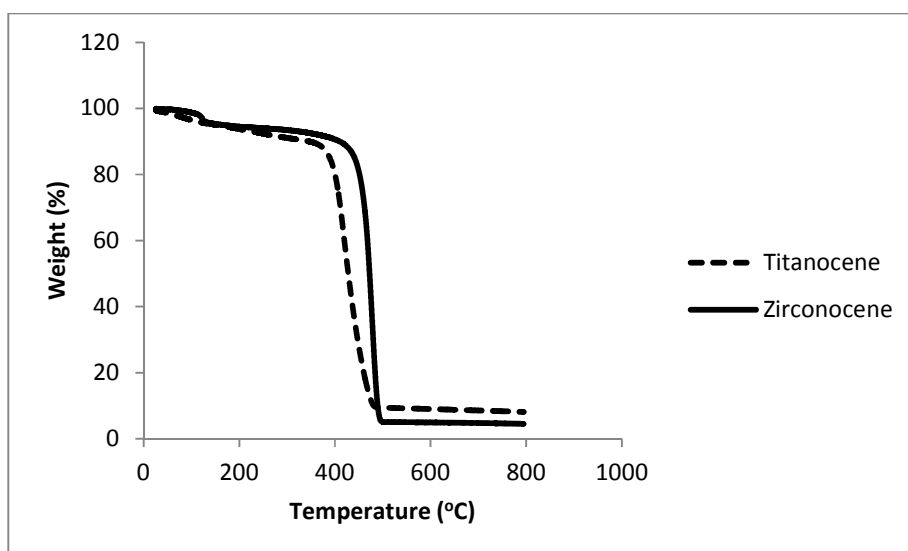


Figure 5-25: TGA curves of polyethylene with doped-titania synthesized at high temperature using different catalysts.

Above figure illustrates the TGA curve of polyethylene nanocomposites synthesized using zirconocene and titanocene at reaction temperature of 60°C. Here, the zirconocene catalyst shows a better thermal stability than the titanocene catalyst, which is due to the fact that molecular weights generally tend to be higher with zirconium catalysts. By analyzing the ash content of these nanocomposites, we could conclude that the ash content represents the filler weight percentage in the polyethylene nanocomposites.

Table 5-6: Experimental Conditions and properties of polyethylene prepared by insitu polymerization using Cp_2ZrCl_2 catalyst and Methyl aluminoxane co-catalyst system.

Entry No.	Filler ^a (in mg)	Pressure (Bar)	Temp. (°C)	Time (minutes)	T _m ^c (°C)	Xc ^c
1	0 ^b	5	30	30	136	67
2	15	5	30	30	137	62
3	15	5	30	60	137	64
4	15	5	30	120	135	71
5	15	2	30	30	130	71

^a TiO₂ doped with Mn, ^b Control, ^c Determined by DSC measurements,

Table 5-6 illustrates the various crystallization behaviors of the polyethylene nanocomposites in reference to the effect of pressure. We reported the DSC thermal analysis in terms of melting temperature (T_m) and degree of crystallinity (Xc). The crystallinity reduces by incorporation of the filler at the ethylene pressure of 5 bar, which

is due to the fact that these filler hinders the crystalline alignment of polymer chain. But with respect to time, we could find that the degree of crystallinity increases due to the decrease in filler to polymer ratio. As far as the melting temperature there is no much variation either by incorporation of filler or by increasing the reaction time at the constant ethylene pressure of 5 bar. At low pressure, we could find that there is a decrease in the melting temperature of the nanocomposite which is due to increase in degree of short chain branching.

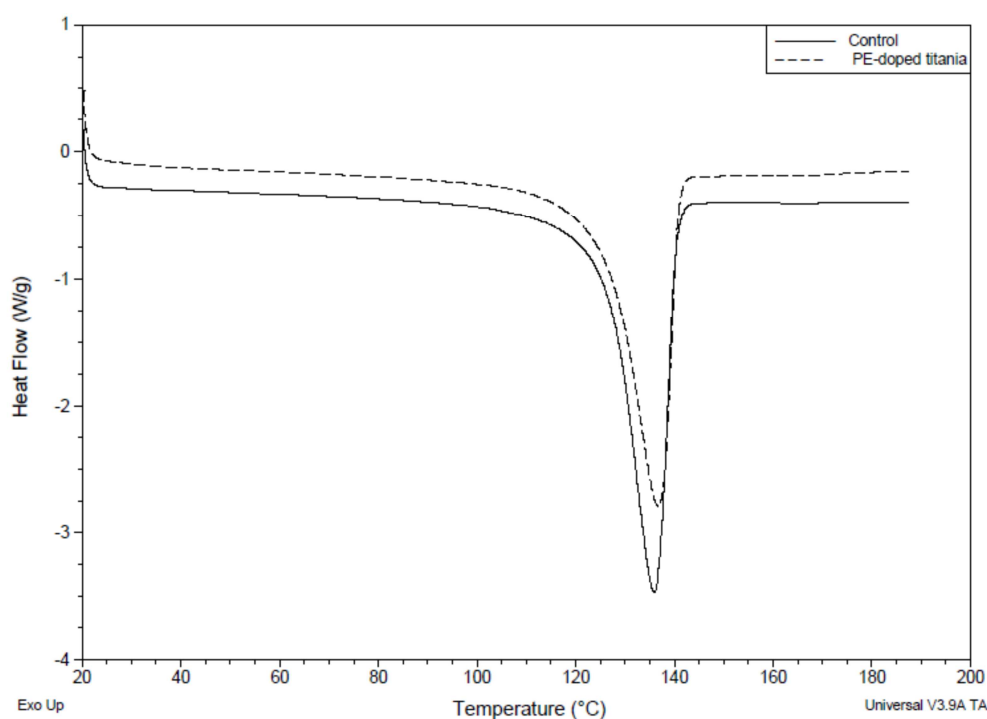


Figure 5-26: DSC second heating curves of homopolymer, polyethylene with doped-titania synthesized at high pressure using Zirconocene catalyst

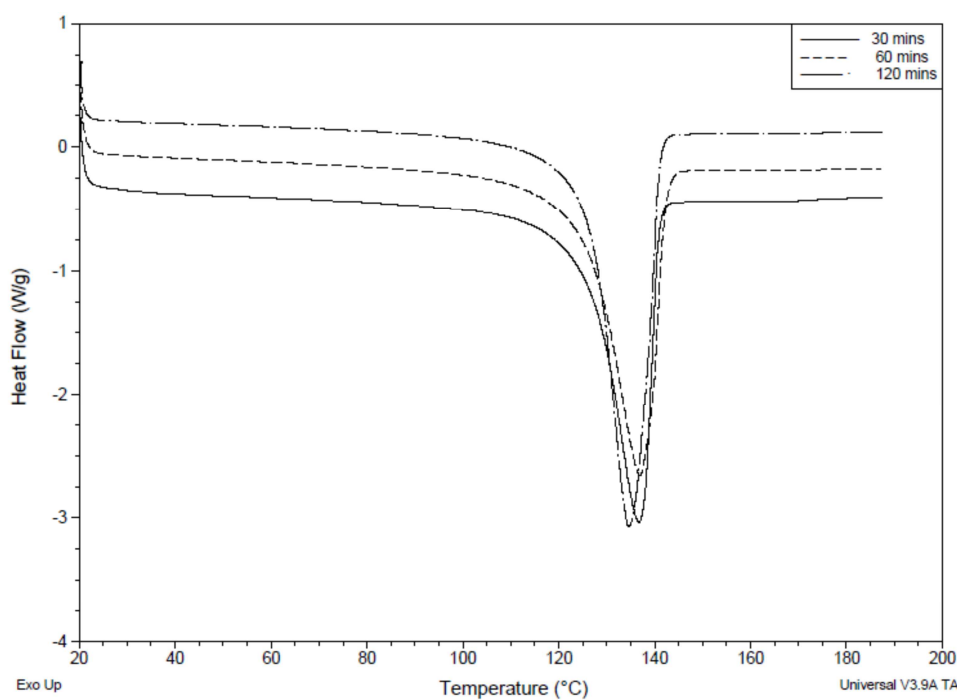


Figure 5-27: DSC second heating curves of polyethylene with doped-titania synthesized at high pressure by varying the reaction time using Zirconocene catalyst

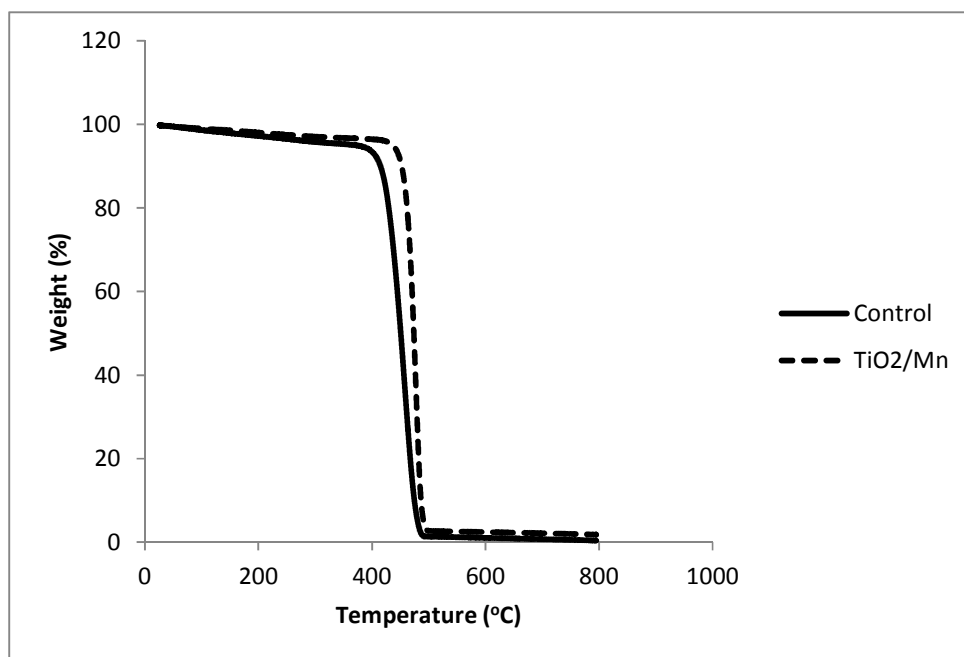


Figure 5-28: TGA curves of homopolymer and polyethylene with doped-titania synthesized at high pressure (5 bar) using Zirconocene catalyst

From above TGA curve, we could find that the thermal stability of polyethylene increases by the addition to doped-titania to the polymer matrix. This variation in the thermal stability alludes to the fact that there is an increase in the molecular weight of the polyethylene by addition of filler. With respect to the ash content, we could find that the ash content for pure homopolymer is almost ground to zero, but in the case of nanocomposite small weight percentage of ash is left out which is due to the filler content in this sample.

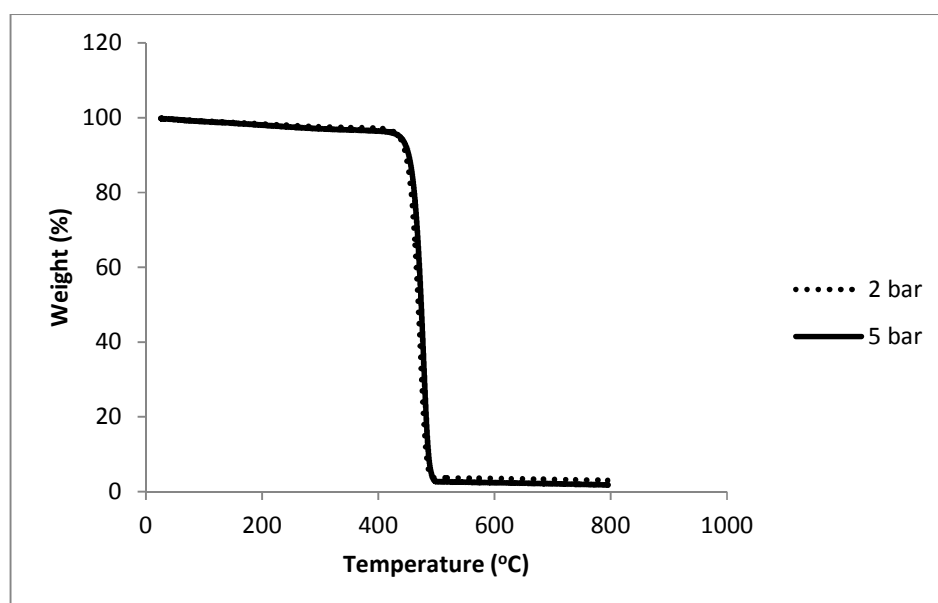


Figure 5-29: TGA curves of polyethylene with doped-titania synthesized at high pressure (5 bar) using Zirconocene catalyst

From Figure 5-29, we conclude that there is an increase in the molecular weight of the synthesized polyethylene nanocomposites with respect to pressure. As here we could see that the thermal stability of nanocomposite synthesized at ethylene pressure of 2 bar is less when compared to the nanocomposite synthesized at 5 bar ethylene pressure. The variation in the ash content is due to the difference in filler weight percentage in these samples.

Mechanical Properties of Polyethylene/doped-titania Nanocomposites

Table 5-7 gives the overall view of mechanical properties of polyethylene/doped-titania nanocomposites, i.e. elastic modulus, ultimate strength, strain at fracture with respect to reaction time. In each case, minimum of five samples were tested and the tabulated values are the average of these results. It can be observed that the elastic modulus and ultimate strength show good enhancement with the addition of filler and this enhancement is further seen with respect to reaction time as well, which is believed to be due to good interface between polymer and TiO_2/Mn thus transferring load from polymer to TiO_2/Mn . It is evident from Table 1 that the filler enhances the mechanical properties of the polyethylene to a great extent as the percentage of strain at fracture increases in multitudes by addition of filler which further increases by the reaction time. This conclusion is very important as these filler not only enhances the activity of the polyethylene by it even enhances the thermal and mechanical properties which widens the application of this filler.

Table 5-7: Ethylene polymerization results at High pressure.^a

Entry No.	Filler	Pressure	Time	Ultimate Strength	Young's Modulus	Strain at Fracture
	(in mg)	(Bar)	(minutes)	(MPa)	(MPa)	(%)
1	0 ^b	5	30	17	325	7
2	15	5	30	17	338	454
3	15	5	60	33	342	1040

^a Polymerization conditions: Solvent toluene = 100 ml, Temp= 30°C, Catalyst (Cp_2ZrCl_2) amount = 20.5 μmol , filler is Mn (1%) doped TiO_2 , $[\text{Al}]/[\text{M}] = 700$, ^b Control,

5.5 Effect of catalyst substituent group on the catalyst activity and thermal properties of polymer in the presence of filler

Cyclopentadienyl ligands are one of the most popular ligands in organometallic chemistry and the development of efficient approaches to the generation of highly substituted or functionalized cyclopentadienyl ligands is of continuing importance [74]. Substitution or functionalization of the cyclopentadienyl ring modifies the steric and electronic properties of the metal center and implies important changes in the structural and chemical behavior of this type of compound [75]. The chemical and physical properties of Group 4 bent metallocenes can be varied over a wide range by modification of the substituent on the cyclopentadienyl ring. One of the main objectives of this work is to study the effect of changing substituent groups (Bu, t-Bu) at the cyclopentadienyl ligand on the catalyst activity and polymer properties.

Table 5-8 shows the results of the polymerization runs carried out using the two catalyst and polymer properties. From the data given in Table 5-8, we can infer that the activity of the catalyst decreases with the increase in the size of substituent group. But in some cases these substituent protects the active polymerization site from deactivation processes [76]. Thus the reason we can find that the activity of Cp_2ZrCl_2 without any substituent group gave less activity compared to the $(\text{BuCp})_2\text{ZrCl}_2$ in the absence of filler. But when the size of the bulky group increases the activity decreases drastically which can concluded by the activity of $(\text{t-BuCp})_2\text{ZrCl}_2$. We also investigated the effect of doped-titania (15 mg) on the activity of these catalyst and the results shows that there is an increase in the

catalyst activity irrespective of the bulky group in the presence of the filler. The increase in the activity of these catalysts is quite low compared with the Cp_2ZrCl_2 , due to the steric effect from the bulky groups present in the cyclopentadienyl ring.

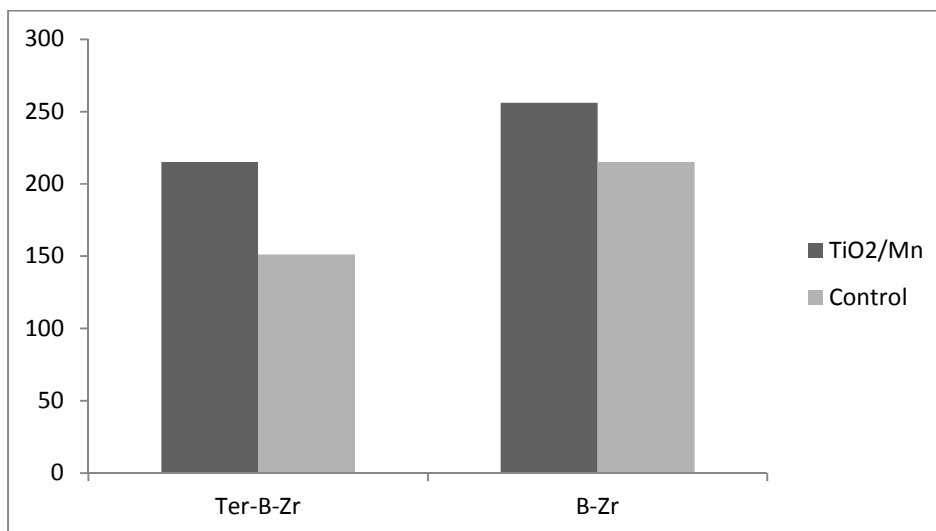


Figure 5-30: Activity of synthesized polyethylene nanocomposites using polymerization time of 30 mins at 30°C in presence of (B-Zr = $(\text{BuCp})_2\text{ZrCl}_2$, Ter-B-Zr = $(t\text{-BuCp})_2\text{ZrCl}_2$).

Thermal properties of Polyethylene/doped-TiO₂ nanocomposites are reported in Table 5-8. A strong correlation was observed between filler loading and the degree of branching in polymer produced as evident in the DSC thermal analysis. We reported the DSC thermal analysis in terms of melting temperature (T_m) and degree of crystallinity (X_c). The melting behavior of polyethylene is mainly related to the short chain branching density.

Increasing short chain branching density decreases lamellar thickness of the crystal structure and thus lowers melting temperature of the polymer. The short chain branching

also affects the degree of crystallinity which is proportional to the fractional amount of crystalline phase in polymer sample [69].

Table 5-8: Experimental Conditions and properties of polyethylene prepared by insitu polymerization using (BuCp)₂ZrCl₂ & (t-BuCp)₂ZrCl₂ catalyst and Methyl aluminoxane co-catalyst system.

Entry No.	Catalyst/Filler ^a (in mg)	Temp. (°C)	Time (minutes)	Activity ^c (°C)	T _m ^d (°C)	Xc ^d	Branches/1000 C ^e
1	A/0 ^b	30	30	215	136	64	4
2	A/15	30	30	256	137	69	5
3	B/0	30	30	153	132	57	11
4	B/15	30	30	215	135	68	10

^a TiO₂ doped with Mn, ^b Control, ^c x 10⁻³ gPE/mol h bar, ^d Determined by DSC measurements, ^e Determined by NMR analysis, Catalyst (A = (BuCp)₂ZrCl₂, B = (t-BuCp)₂ZrCl₂)

It can be observed from Table 5-8 that at the optimal concentration of filler loading (15 mg) there isn't much difference in the melting temperature in the butyl zirconium catalyst compared to the control which is due to the similarity in the degree of short chain branching, which symbolize that the promoter effect of filler doesn't affect the thermal property to a great extent. But in the case of ter-butyl zirconium catalyst, the melting temperature is slightly lower than the butyl catalyst which corresponds to the increase in the short chain branching. The crystallinity increases with the addition of doped-titania to the polyethylene matrix, and the crystallinity of ter-butyl zirconium catalyst is comparatively less than the butyl catalyst, this factor is due to the difference in degree of short chain branching given the table.

The above results also shows that the presence of small amounts of filler in PE/doped-TiO₂ nanocomposites will enhance the crystallinity of PE, which shows that the dispersed doped-TiO₂ particles act as nucleating agents for PE crystallization as it offers more sites for crystal growth in the matrix. Figure 5-31-5-33 represents the second heating curve obtained from DSC analysis.

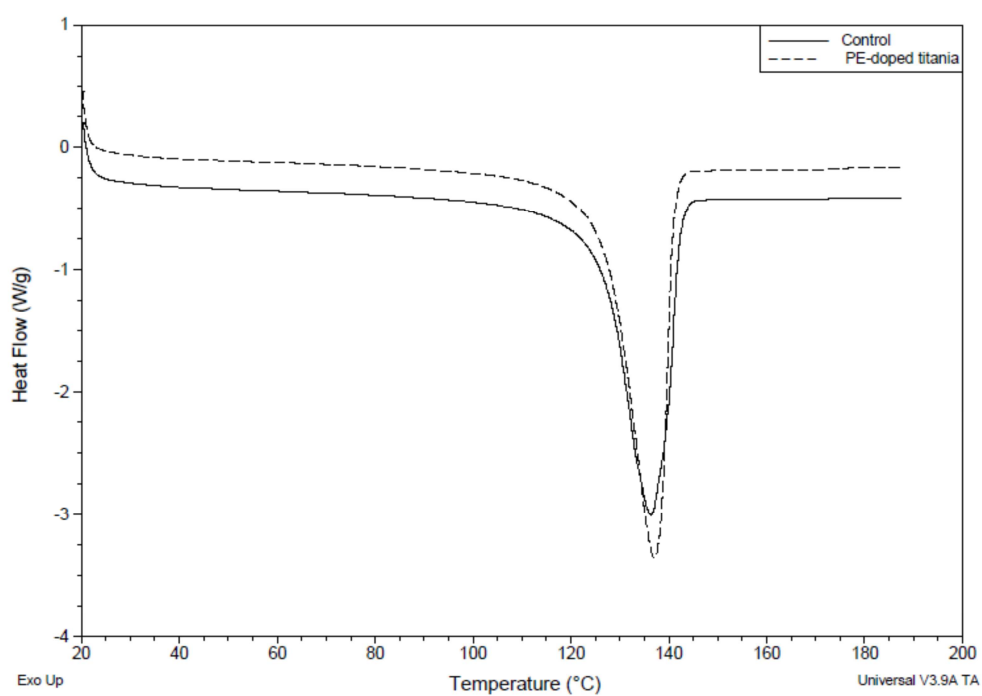


Figure 5-31: DSC second heating curves of homopolymer, polyethylene with doped-titania synthesized using butyl-Zirconocene catalyst

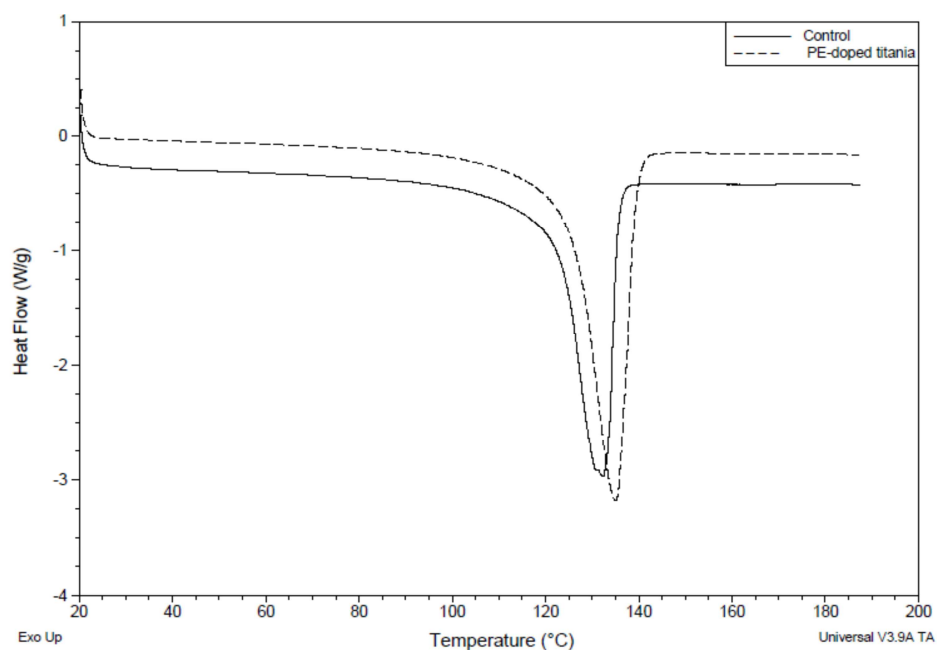


Figure 5-32: DSC second heating curves of homopolymer, polyethylene with doped-titania synthesized using ter-butyl-Zirconocene catalyst

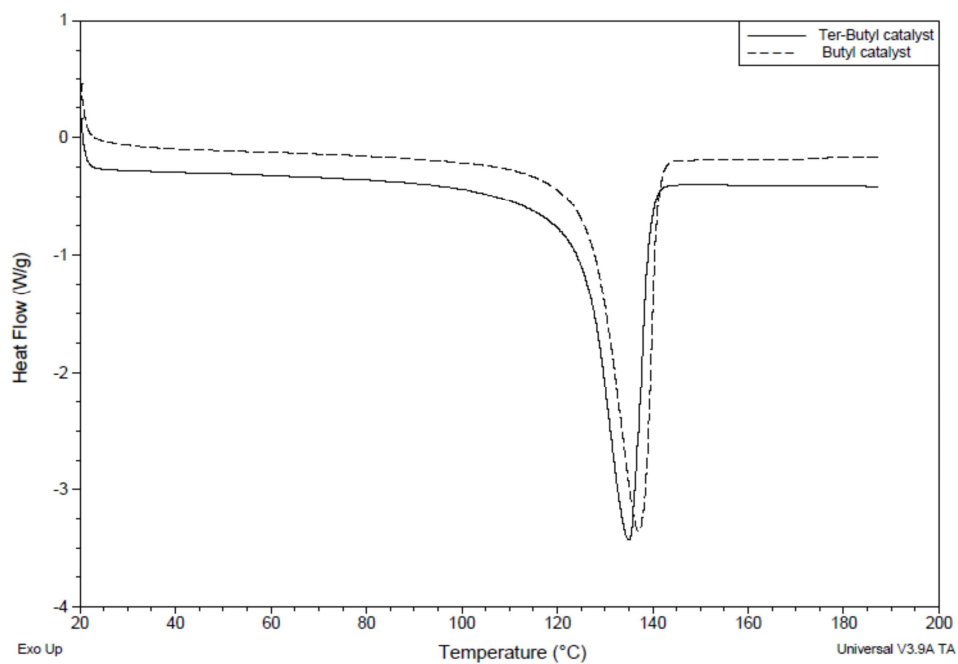


Figure 5-33: DSC second heating curves of polyethylene with doped-titania synthesized using butyl and ter-butyl-Zirconocene catalyst

In case of TGA curves which are shown in the below figures, thermal stabilization of all the nanocomposites and the fraction of volatile components are observed under inert nitrogen atmosphere.

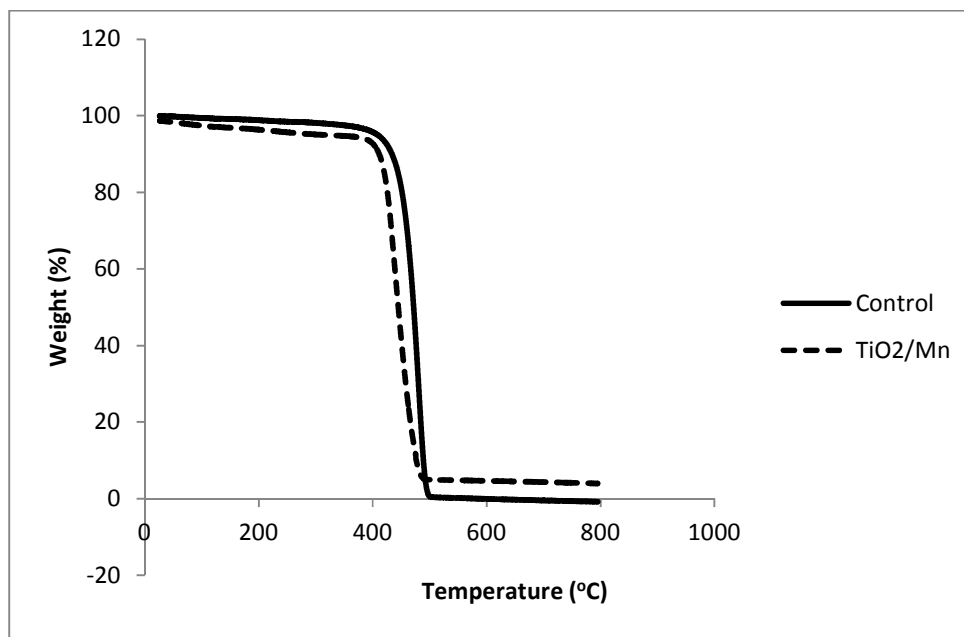


Figure 5-34: TGA curves of homopolymer, polyethylene with doped-titania synthesized using butyl-Zirconocene catalyst

From the Figure 5-34, its clear that the thermal stability of polyethylene nanocomposite with doped-titania is comparatively less than the homopolymer, this is due the difference in their molecular weight. The degradation temperature decreases by addition of filler to the polymer matrix. When we analyze the ash content, which is the amount of metal catalyst in the material. It is usually assumed that upon completion of TGA, all carbon has been removed in the forms of CO and CO₂ and that all remaining material consists of metal oxides. In the case of polyethylene/doped-titania nanocomposite less ash is found which is due to the polymer to filler ratio, since the activity in the presence of doped-titania is high, the filler weight percentage is low which corresponds to less ash content in the TGA curves.

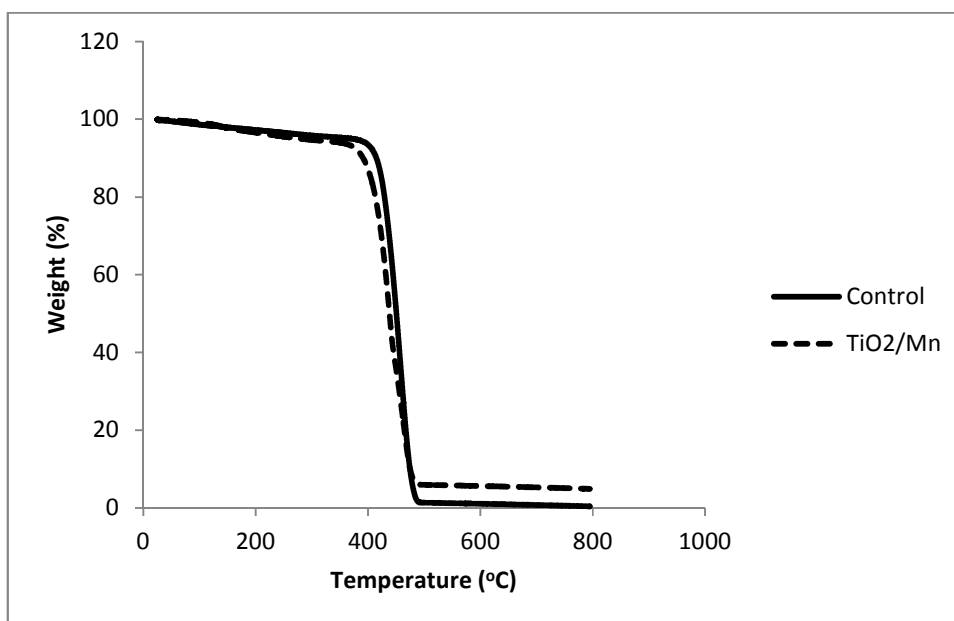


Figure 5-35: TGA curves of homopolymer and polyethylene with doped-titania synthesized using ter-butyl-Zirconocene catalyst

From Figure 5-35, it is very apparent that the thermal stability of polyethylene/doped-titania nanocomposite synthesized using the ter-butyl-zirconocene catalyst follows the same trend like that of butyl catalyst.

From the below figure, it clear that the thermal stability of nanocomposite synthesized using ter-butyl catalyst is lower than the nanocomposite synthesized using butyl catalyst, this corresponds to the molecular weight of these polyethylene nanocomposites. Its known from te literature, that the ter-butyl catalyst yields polyethylene with less molecular weight compared to the butyl catalyst. When we investigate the ash content, we could find that the ash content corresponds to the filler weight percentage in these samples, thus, when the activity is less then filler weight percentage will be more. The ash content in the case of ter-butyl nanocomposite is higher than the butyl catalyst due to the filler weight percentage.

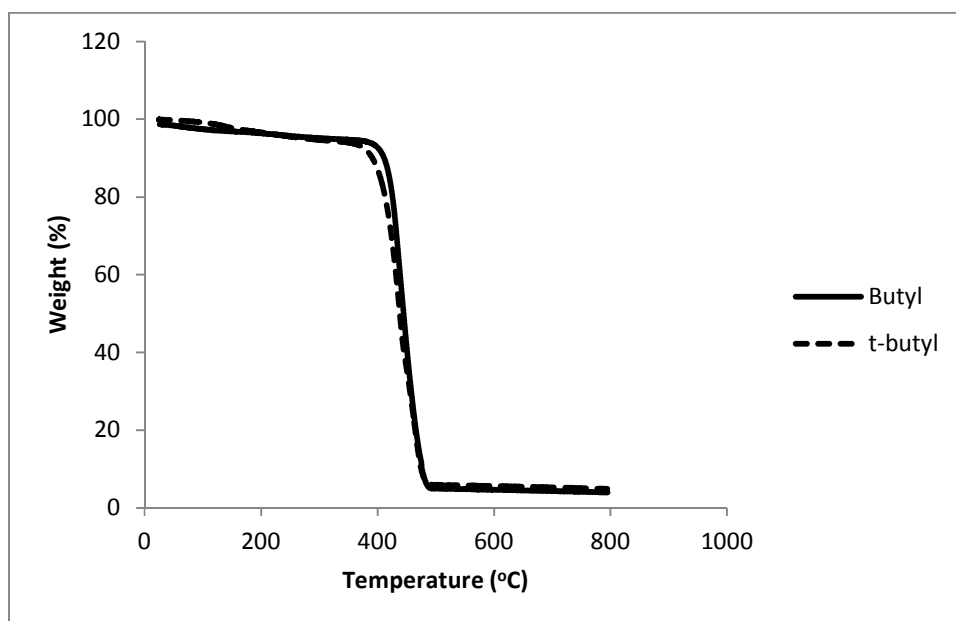


Figure 5-36: TGA curves of polyethylene with doped-titania, synthesized using butyl and ter-butyl-Zirconocene catalyst

5.6 Effect of Polymerization Conditions on the catalyst activity and thermal properties of polymer in the presence of filler

The effects of reaction temperature on catalyst activity and thermal properties were very clear from the experimental data. There was a decrease in the melting temperature of Zirconocene in the presence of filler at 60°C of polymerization temperature due to the increase in degree of short of branching. This temperature effect on activity was observed by maintaining the ethylene pressure at 1 bar and by varying reaction temperature as shown in Table 5-9

Table 5-9: Experimental Conditions and properties of polyethylene prepared by insitu polymerization using Cp_2ZrCl_2 & Cp_2TiCl_2 catalyst and Methyl aluminoxane co-catalyst system.

Entry No.	Catalyst/Filler ^a	Temp. (°C)	Time (minutes)	Activity ^c	T _m ^d (°C)	Xc ^d	Branches/1000 C ^e
	(in mg)	(°C)	(minutes)		(°C)		
1	A/0 ^b	30	30	215	136	64	4
2	A/15	30	30	256	137	69	5
3	A/0	60	30	255	131	62	n.d ^f
4	A/15	60	30	234	132	69	n.d
5	B/0	30	30	153	132	57	11
6	B/15	30	30	215	135	68	10
7	B/0	60	30	209	131	63	n.d
8	B/15	60	30	159	127	74	n.d

^a TiO₂ doped with Mn, ^b Control, ^c x 10⁻³ gPE/mol h bar, ^d Determined by DSC measurements, ^e Determined by NMR analysis, ^f not determined, Catalyst (A = (BuCp)₂ZrCl₂, B = (t-BuCp)₂ZrCl₂)

From figure 5-37, it is evident that there is an increase in the catalytic activity of butyl-zirconocene with the increase in the polymerization temperature in the absence of filler, this phenomenon is due to the increase in the chain propagation rate which will in turn increase the activity of the catalyst. Though there is an increase in the catalytic activity at 60°C in the absence of filler (255×10^3 gPE/mol Zr h bar), but its lower than the activity at 30°C in the presence of filler (456×10^3 gPE/mol h bar). A similar trend was found even with ter-butyl catalyst. The activity is high in the presence of filler at 30°C (215×10^3 gPE/mol h bar) compared to control even at 60°C (209×10^3 gPE/mol h bar).

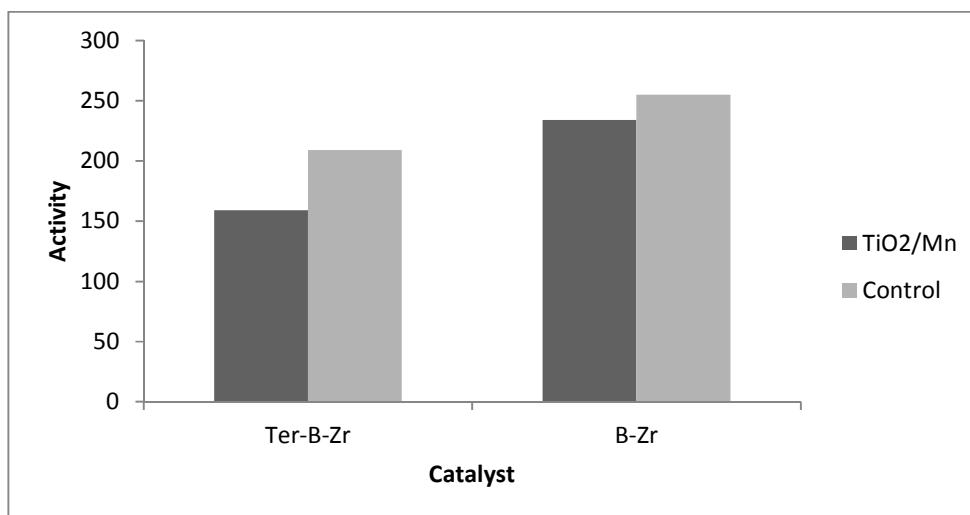


Figure 5-37: Activity of synthesized polyethylene nanocomposites using polymerization time of 30 mins at 60°C in presence of (B-Zr = $(\text{BuCp})_2\text{ZrCl}_2$, Ter-B-Zr = $(\text{t-BuCp})_2\text{ZrCl}_2$).

From the given figure, we are able to infer that the activity of the catalyst decreases with the increase of the reaction temperature in presence of filler. The low yield as a result of the filler addition could be due to more steric hindrance arising from the nanoparticles and strong interaction might have happened between the filler and the co-catalyst [44]. This decrease in activity may be due to deactivation of active sites.

From Table 5-9, it is evident that the decrease in temperature increases the melting temperature in the case of both the catalyst in the presence of doped-titania, this trend showed a reduction in the short chain branch content due to the dominance of chain propagation over chain walking reactions at such conditions [69]. It seems that the nanocomposite synthesized using butyl catalyst has less short chain branching compared to the ter-butyl catalyst which is evident through the melting temperature. The melting behavior of PE is mainly related to short chain branching density. An increase in short chain branching density decreases the lamellar thickness of crystal structure thereby lowers the melting temperature of polymer. The effect of filler had the same effect on crystallinity just like pure zirconocene catalyst irrespective of the temperature. Figure 5-38-5-39 represents the second heating curve obtained from DSC analysis.

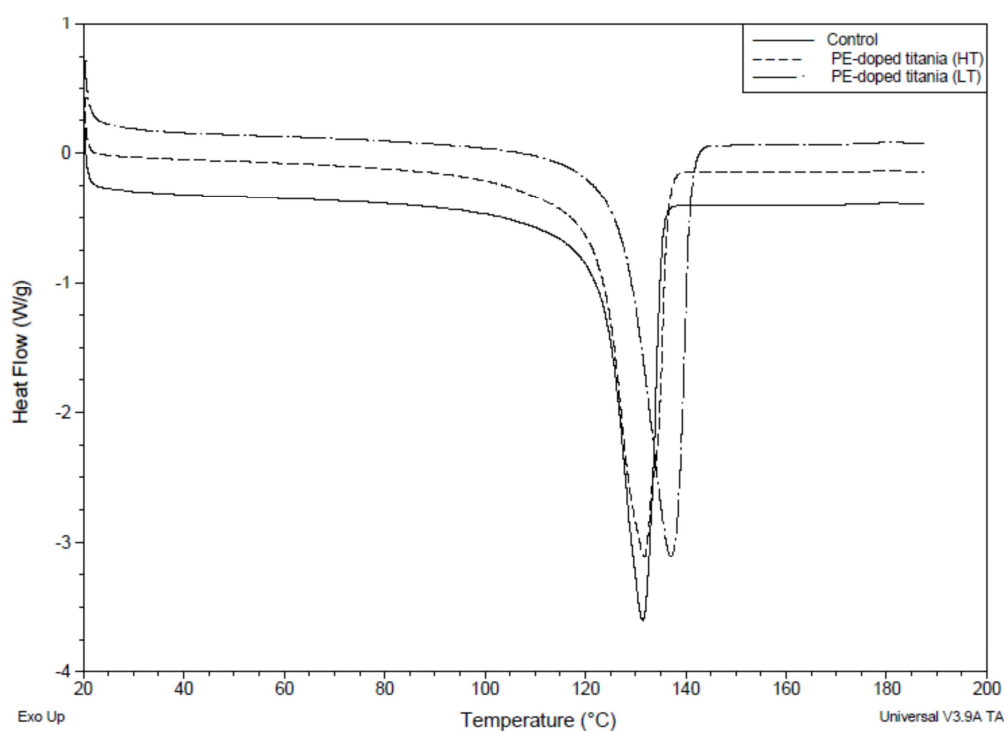


Figure 5-38: DSC second heating curves of homopolymer synthesized at high temperature, polyethylene with doped-titania synthesized at high temperature and low temperature using butyl-Zirconocene catalyst

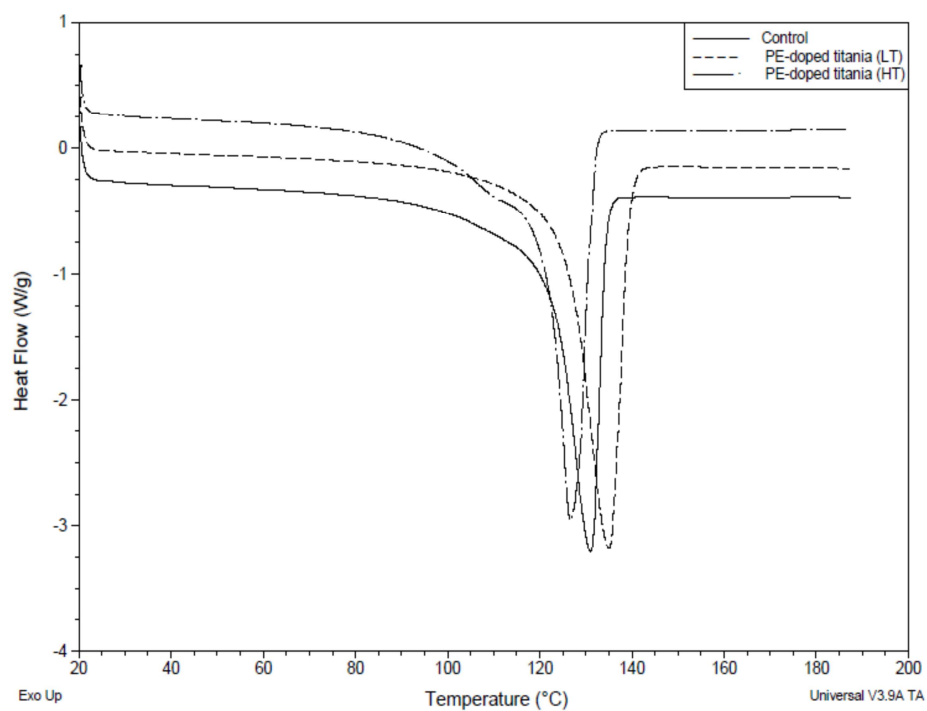


Figure 5-39: DSC second heating curves of homopolymer synthesized at high temperature, polyethylene with doped-titania synthesized at high temperature and low temperature using butyl-Zirconocene catalyst

In Figure 5-39, we could find that the polyethylene nanocomposite synthesized at high temperature shows a broad melting peak, this observation could be attributed to more irregularity of the chain structure of the polyethylene produced by ter-butyl catalyst.

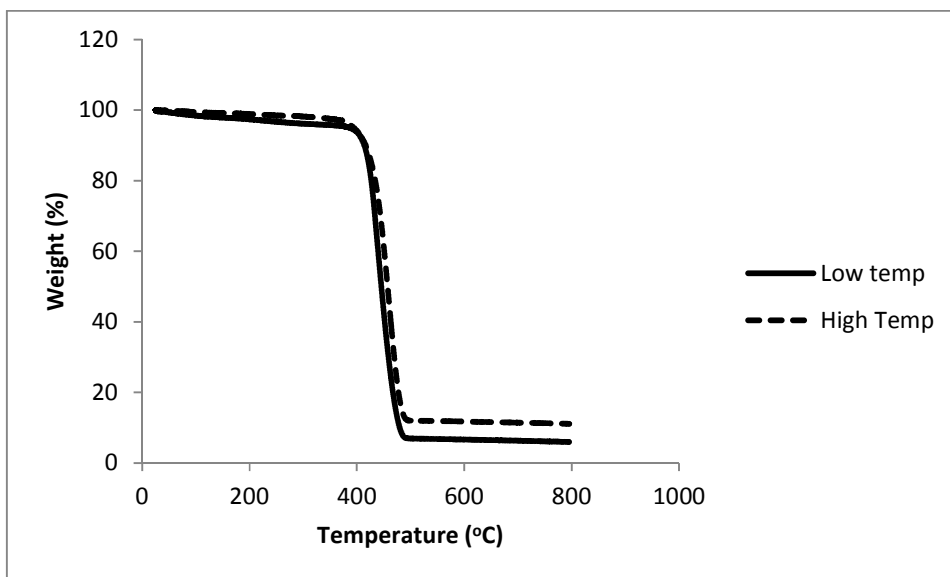


Figure 5-40: TGA curves of polyethylene with doped-titania synthesized at different polymerization temperatures using Butyl-Zirconocene catalyst

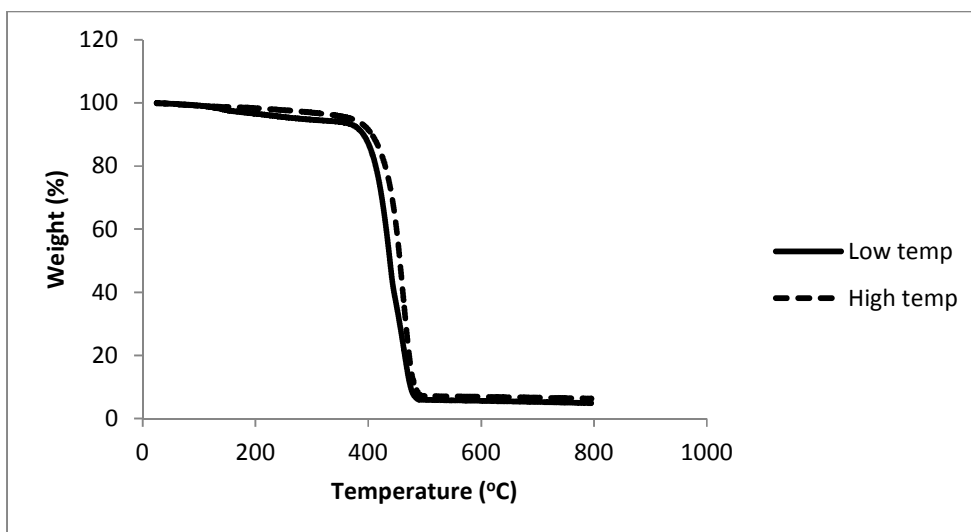


Figure 5-41: TGA curves of polyethylene with doped-titania synthesized at different polymerization temperatures using ter-Butyl-Zirconocene catalyst

From the TGA analysis of polyethylene nanocomposites we could infer that the thermal stability of polyethylene increases with the temperature as the degradation temperature of polyethylene nanocomposites synthesized at high temperature higher than the degradation temperature of polyethylene nanocomposites synthesized at low temperature. This increase in the degradation temperature is due to the increase in the molecular weight of these sample, but it known that as the temperature increases further there will be decrease in the thermal stability due to the decrease in molecular weight which will show the predominance of chain transfer reaction at high temperature.

There is a difference in the ash content of these polyethylene nanocomposites which is due to the filler weight percentage. As we discussed in the previous sections, the activity of the catalyst was low at high temperature which means less yield of polyethylene was obtained. The weight percentage of filler is more when the polyethylene nanocomposites are synthesized at high temperature thus there is an increase in ash content.

5.7 Effect of filler on activity of Zeigler Natta Catalyst and polymer properties

From Table 5-10, we could find that the activity of Zeigler-Natta catalyst is very low irrespective of temperature. This fact has been proven in the literature by concluding that the activity of Zeigler-Natta catalyst is low compared to the activity of metallocene catalyst. When we investigate the effect of doped-titania on the catalytic activity, we could find that the activity of the catalyst is reduced at low temperature by the presence of filler, this might be due to the steric hindrance from the filler and the interaction between the filler and co-catalyst plays a vital role.

Table 5-10: Experimental Conditions and properties of polyethylene prepared by insitu polymerization using TiCl_4 catalyst and Tri-isobutyl aluminum co-catalyst system.

Entry No.	Filler ^a (in mg)	Temp. (°C)	Time (minutes)	Activity ^c	T _m ^d (°C)	Xc ^d
1	0 ^b	30	30	26	136	61
2	15	30	30	35	135	65
3	0	60	30	7	136	70
4	15	60	30	2	136	60

^aTiO₂ doped with Mn, ^b Control, ^c x 10⁻³ gPE/mol h bar, ^dDetermined by DSC measurements,

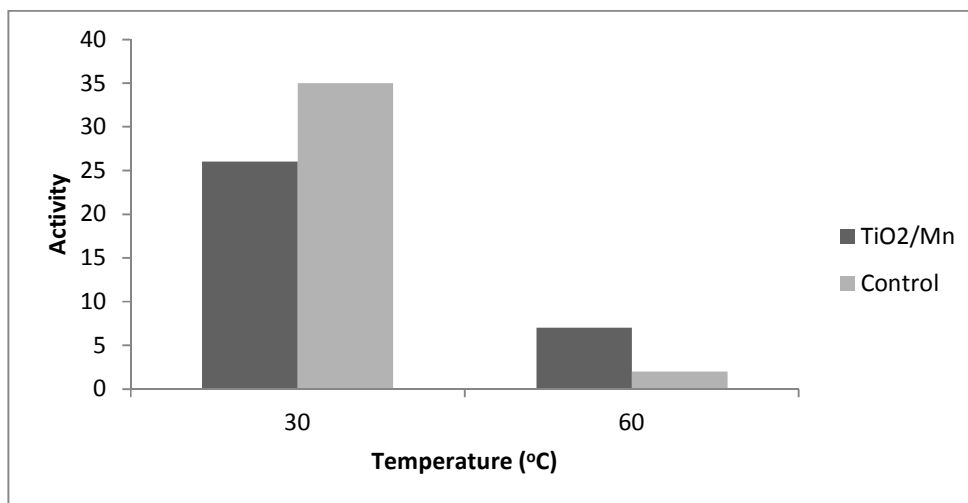


Figure 5-42: Activity of synthesized polyethylene nanocomposites using polymerization time of 30 mins at different temperatures in presence of Zeigler-Natta catalyst.

When the reaction temperature is increased we could find that there is an increase in the activity in presence of filler, this is due to the increase in chain propagation rate constant in presence of filler. The melting temperature is not affected to a great extent by addition of filler but we could find that there is a difference in the crystallinity of these polymers in the presence of filler.

Chapter 6

Conclusion and Future Work

Ethylene polymerization was carried out using metallocene catalysts (Cp_2ZrCl_2 and Cp_2TiCl_2) activated with MAO in the presence of Mn doped titania. We investigated the effects of concentration of filler, ethylene pressure and reaction temperature on the catalyst activity and polymer properties. The optimal concentration of filler in the polymerization was found to be 15 mg, where there was a four-fold increase in the catalytic activity of Cp_2ZrCl_2 at 30°C. There was also increase in the catalytic activity of Cp_2TiCl_2 in the presence of filler. The molecular weight of the polyethylene was found to be low in the presence of optimal concentration of filler though it enhances the catalytic activity. The morphology indicates spherical particle which in turn shows the nucleation effect of the filler. The raise in reaction temperature hindered the catalytic activity in the presence of filler which might be due to the steric hindrance from the nanoparticles. The effect of pressure was as expected, the activity of catalyst increased with pressure since more monomers were exposed to active site of the catalyst. The thermal and mechanical properties were analyzed. The effect of substituent group in the zirconocene catalyst was also studied by using $(\text{BuCp})_2\text{ZrCl}_2$ & $(\text{t-BuCp})_2\text{ZrCl}_2$. In this study we concluded that the effect of filler on activity of these was same as like the pure zirconocene catalyst. The steric effect from the substituent groups had a drastic impact on the activity of the catalyst.

6.1 Future Research

The polymer industry in Saudi Arabia is one of the biggest industries in the world and it is expanding very fast. Nanotechnology science is one of the promising and attractive areas that it will significantly affect our daily life. Application of nanotechnology to the polymer research is very interesting and worth to the industry scale. Following are some of the recommendations for any future work to be done:

1. The effect of filler can be analyzed in various other homopolymer and copolymer system.
2. The effect of filler on the activity of other catalyst like nickel, vanadium catalyst can be analyzed.
3. The effect of temperature can be further analyzed by reducing the temperature below 30°C and its effect on the activity of the catalyst and polymer properties can be investigated.
4. The effect of filler on the activity of catalyst with different substituent groups can be analyzed and the polymer obtained through these catalysts can be further investigated in detail.

Bibliography

1. Zou. H., Wu. S.S., Shen. Chem. Rev. 2008, 108, 3893-3957.
2. Kontou E, Niaounakis M Polymer, 2006 47, 1267–1280.
3. Li KT, Dai CL, Kuo CW Catal Commun, 2007, 8, 1209–1213.
4. Jongsomjit B, Chaichana E, Prasertthdam P J Mater Sci, 2005, 40, 2043–2045.
5. Chaichana E, Jongsomjit B, Prasertthdam P Chem Eng Sci, 2007, 62, 899–905.
6. Nussbaumer RJ, Caseri WR, Tervoort PT, Macromol Mater Eng, 2003, 288, 44–49.
7. Wang Z, Li G, Xie G, Zhang Z Macromol Chem Phys, 2005, 206, 258–262.
8. Chen XD, Wang Z, Liao ZF, Mai YL, Zhang MQ Polym Test, 2007, 26, 202–208.
9. Owpradit W, Jongsomjit B Mater Chem Phys, 2008, 112, 954–961.
10. Kuo MC, Tsai CM, Huang JC, Chen M Mater Chem Phys, 2005, 90, 185–195.
11. Desharun C, Jongsomjit B, Prasertthdam P, Catal Commun, 2005, 9, 522–528.
12. Jongsomjit B, Panpranot J, Okada M, Shiono T, Prasertthdam P Iran Polym J, 2006, 15, 431–437.
13. Jongsomjit B, Panpranot J, Prasertthdam P, Mater Lett, 2007, 61, 1376–1379.
14. Thomas Hanemann and Dorothee, Materials, 2010, 3, 3468-3517 .
15. Wagner. D., Vaia. R., Nanocomposites: issues at the interface. Materials Today, 2004.
16. Jordan. J., Jacobb. K., Tannenbaumc. R., Sharafb. M., Jasiukd. I., Materials Science and Engineering A 2005, 393, 1.
17. Jancar. J, Douglas. J. F., Starr. F.W., Kumar. S. K., Cassagnau. P., Lesser. A. J., Sternstein. S. S., Buehler. M. J., Polymer 2010, 51, 3321.
18. Jeon. I.Y., Baek. J. B., Materials 2010, 3, 3654.
19. Su. H.W., Chen.W.C., Macromol. Chem Phys. 2008, 209, 778–1786.

20. Klaus Friedrich, Stoyko Fakirov, and Zhong Zhang, Springer, 2005.
21. Akita,H.; Hattori, T.; J. Polym. Sci. B: Polym. Phys., 37, 189, 1999.
22. Mark, J. E.; Polym. Eng. Sci., 36, 24, 1996.
23. Jordan, J.; Jacob, K. I.; Jasink, I.; Materi. Sci. Eng. A., 393, 1, 2005.
24. Park, C. I.; Park, O. O.; Kim, H. J.; Polymer, 42, 7465, 2001.
25. Y.S. Thio, A.S. Argon, R.E. Cohen, M. Weinberg, Polymer 43, (2002), 3661.
26. A.L.N. da Silva, M.C.G. Rocha, M.A.R. Moraes, C.A.R. Valente, F.M.B. Coutinho, Polym. Test. 21, (2002), 57.
27. A. Tabtiang, R. Venables, Eur. Polm. J. 36, (2000), 137.
28. C.M. Chan, J.S. Wu, J.X. Li, Y.K. Cheung, Polymer 43, (2002), 2981.
29. J. Gonzalez, C. Albano, M. Ichazo, B. Diaz, Eur. Polym. J. 38 ,(2002), 2465.
30. P. Supaphol, W. Harnsiri, J. Junkasem, J. Appl. Polym. Sci 92. (2004) 201.
31. S. Miao, Appl. Surf. Sci. 220, (2003), 298.
32. T.J. Turton, J.R. White, Polym. Degrad. Stab. 74, (2001),559.
33. G.I. Titelman, Y. Gonen, Y. Keider, S. Bron, Polym.Degrad. Stab. 17, (2002), 345.
34. Z. Wang, X.Wang, G. Xie, G. Li, Z. Zhang Composite Interfaces, 13, (2006), 623.
35. P. Supaphol, P. Thanomkiat, J. Junkasem, R. Dangtungee Polymer Testing 26, (2007), 20.
36. Kaminsky. W, Funck. A, Macromol. Symp. 2007, 260, 1.
37. Sandler. J., Broza. K. G., Nolte. M., Schulte. K., Lam. Y. M., Shaffer. M. S. P., J. Macromol. Sci. B 2003, 42, 479.
38. Sinclair. K. B., Macromol. Symp. 2001, 173, 237.
39. Boor, J. ‘Ziegler-Natta Catalysts and Polymerizations’, Academic Press, New York, 1979.
40. Sinn, H. and Kaminsky, W. 1980 Ad.Organomet. Chem. 18: 99.
41. Keii, T. ‘Kinetics of Ziegler-Natta Polymerization’, Kodansha Ltd, Tokyo, 1972.

42. Ghoi .J. H., Chung .J. S., Shin .H. W., Song, I. K. and Lee, W. Y. 1996. Eur. Polym. J. 32: 405-410.
43. Galli .P. and Vecellio .G. 2001. Prog. Polym. Sci. 26: 1287-1336.
44. Rong .J. F, Li .H. Q, Jing .Z. H, Hong .X. Y., Sheng M 2001 J Appl Polym Sci 82:1829.
45. Jin .Y. H., Park .H. J., Im .S. S., Kwak .S. Y., Kwak .S. J., 2002 Macromol RapidCommun 23:135.
46. Yang .F., Zhang .X. Q., Zhao .H. C., Chen .B., Huang .B. T., Feng .Z. L., 2003 J Appl Polym Sci 89:3680.
47. Ahmad Ramazani S. A., Fahimeh Tavakolzadeh, 2008, Poly. Sci. Tech, 274:65-71.
48. Ahmad Ramazani S. A., Fahimeh Tavakolzadeh, Hossein Baniasadi, 2010, Appl Polym Sci, 115:308-314.
49. Yingjuan Huang, Yawei Qin, Yong Zhou, Hui Niu, Zhong-Zhen Yu, Jin-Yong Don, 2010, Chem. Mater., 22: 4096–4102.
50. Parvatikar, N.; Ambika Prasad, M. V. N. J. Appl. Polym. Sci. 2006, 100, 1403-1405.
51. Badheka, P.; Magadala, V.; Gopi Devaraju, N.; Lee,B. I.; Kim, E. S. J. Appl. Polym. Sci. 2006, 99, 2815-2821.
52. Schroeder, R.; Majewski, L.; Grell, M. AdV. Mater. 2005, 17, 1535-1539.
53. Ger. 3240382 (1984), A. G. Hoechst, invis.: W. Kaminsky, J.Dutschke, H. Maedler, M. Miri and M. Schlobohm, Chem. Abstr., 101, 11564k (1984).
54. W. Kaminsky, Macromol. Chem. Phys., 197, 3907 (1996).
55. W. Kaminsky and F. Renner, Makromol. Chem., Rapid. Commun.,14, 239 (1993).
56. P. Ross, G. B. Meier, J. J. C. Samson, G. Weickert and K. R. Westerterp, Macromol. Rapid Commun., 18, 319 (1997).
57. P. Kumkaew, S. E. Wanke, P. Prasertthdam, C. Danumah and S. Kaliaguine, J. Appl. Polym. Sci., 87, 1161 (2003).
58. K. Tannous and J. B. P. Soares, Macromol. Chem. Phys., 203, 1895 (2002).

59. N. Guo, S.A. DiBenedetto, Do-Kyun Kwon, L. Wang, M.T. Russell, M.T. Lanagan, A. Facchetti, T.J. Marks *J. Am. Chem. Soc.* (2007), 129, 766-767.
60. W. Owpradit, B. Jongsomjit. *Mater Chem Phys* (2008), 112, 954.
61. W. Owpradit, O. Mekasuwandumrong, J. Panpranot, A. Shotipruk, B. Jongsomjit *Polym. Bull.* 2010.
62. B. Hojjati, P. A. Charpentier *Polymer* (2010), 51, 5345
63. W. Kaminsky, *J. Chem. Soc., Dalton Trans.* 1998, 1413.
64. Owpradit W, Jongsomjit B *Mater Chem Phys.* 2008 112:954–961
65. G. G. Hlatky, *Coord. Chem. Rev.* 1996, 181, 243.
66. K. K. Kang, J. K. Oh, Y. T. Jeong, T. Shiono, T. Ikeda, *Macromol. Rapid Commun.* 1999, 20, 308.
67. L. Vaisman, H. D. Wagner and G. Marom, *Adv. Colloid Interface Sci.* 2006, 37, 128.
68. B. Jongsomjit, E. Chaichana, P. Praserttham, *J. Mater. Sci.* 2005, 40, 2043.
69. F. AlObaidi, Z. Ye, S. Zhu, *Polymer*, 2004, 45, 6823-6829.
70. P. Sracck, P. Lehmus, J. V. Seppala, *Polym. Eng. Sci.* 1999, 39, 1444.
71. J. Nieto, T. Oswald, F. Blanco, J. B. P. Soares, B. Monrabal, *J. Polym. Sci. Part. B: Polym. Phys.* 2001, 39, 1616.
72. J. B. P. Soares, S. Anantawaraskul, *J. Polym. Sci. Part. B: Polym. Phys.* 2005, 43, 1557.
73. L. J. D. Britto, J. B. P. Soares, A. Penlidis, B. Monrabal, *J. Polym. Sci. Part. B: Polym. Phys.* 1999, 37, 539.
74. M. Hobi, O. Ruppert, V. Gramlich, A. Togni, *Organometallics.* 1997, 16, 1384.
75. R.W. Heo, F.B. Somoza, T.R. Lee, *J. Am. Chem. Soc.* 1998, 120, 1621.
76. Neil E. Grimmer, Neil J. Coville, Charles B. de Koning, *J. Organomet. Chem.* 2002, 642, 195

Curriculum Vita

Abdul Kaleel Sulaiman Haniffa

- **Email:** abdulkbasis@gmail.com
- **DOB:** 18/04/1986
- **Nationality:** Indian
- **Parmament Address:** No.1/35, Deivasigamani Street, Chennai, INDIA – 600094
- **Contact No:** 0535042857

Education

- Masters (M.S) in Chemical Engineering, Chemical Engineering department, KFUPM, Dhahran, Saudi Arabia - 2009 to 2011.
- Bachelors of Technology (B.E) in Industrial Biotechnology, IBT department, Anna University, Chennai, India – 2003 to 2007.

Research Interests

- Polymer Reaction Engineering
- Polymer composites